CORRESPONDING EDITOR:

Stephanie C. Herring, PhD
NOAA National Climatic Data Center
325 Broadway, E/CC23, Rm 1B-131
Boulder, CO, 80305-3328
E-mail: stephanie.herring@noaa.gov

COVER CREDITS:

FRONT: The final wave of rain storms make their way through Boulder, Colorado, bringing another day of flooding to the already rain swollen area, 15 September 2013. Image by ©Ed Endicott/Demotix/Corbis.

BACK: The city of Boulder, Colorado, experienced substantial flooding for four days that have lasting effects, 18 September 2013. Image by ©Anna M Weaver/Demotix/Corbis.

HOW TO CITE THIS DOCUMENT

Citing the complete report:

Herring, S. C., M. P. Hoerling, T. C. Peterson, and P. A. Stott, Eds., 2014: Explaining Extreme Events of 2013 from a Climate Perspective. *Bull. Amer. Meteor. Soc.*, **95** (9), S1–S96.

Citing a section (example):

Hoerling, M., and Coauthors, 2014: Northeast Colorado extreme rains interpreted in a climate change context [in "Explaining Extremes of 2013 from a Climate Perspective"]. *Bull. Amer. Meteor. Soc.*, **95** (9), S15–S18.

EDITORIAL AND PRODUCTION TEAM

6. SEASONAL AND ANNUAL MEAN PRECIPITATION EXTREMES OCCURRING DURING 2013: A U.S. FOCUSED ANALYSIS

Thomas R. Knutson, Fanrong Zeng, and Andrew T. Wittenberg

The Coupled Model Intercomparison Project phase 5 model analyses suggest that seasonal and annual mean precipitation extremes occurring during 2013 in north-central and eastern U.S. regions, while primarily attributable to intrinsic variability, were also partly attributable to anthropogenic and natural forcings combined.

Introduction. We analyze several U.S. regions with seasonal and annual mean precipitation anomalies in 2013 that we classify as "extreme" (i.e., ranked first, second, or third highest or lowest). Our analysis uses the Global Historical Climatology Network (GHCN) monthly precipitation dataset (Vose et al. 1992), covering 1900–2013, on a 5° × 5° grid effectively limited to land regions. The extremes are analyzed in the context of long-term climate change, using trend analysis of historical and control run experiments from 23 Coupled Model Intercomparison Project phase 5 (CMIP5) models (Supplemental Material; Taylor et al. 2012).

Where did seasonal and annual mean precipitation extremes occur in 2013? Figure 6.1a–e identifies several regions of the continental United States that experienced record or near-record seasonal or annual mean precipitation anomalies during 2013. Global maps of seasonal and annual anomalies, and their associated extreme occurrences for 2013 (Supplementary Fig. S6.1), show that record or near-record wet and dry anomalies for 2013 were well dispersed around the globe. Supplementary Fig. S6.2 shows that in recent decades, annual mean rainfall has shown greater areal coverage for record or near-record annual mean wet extremes than dry extremes. In contrast, recent seasonal and annual mean surface temperatures are much more strongly skewed toward warm extremes (e.g., Knutson et al. 2013a).

We focus on six U.S. regions in this study (Fig. 6.1; Supplementary Fig. S6.1) including: the "northern tier—ANN (annual);" "upper Midwest—MAM (March–May);" "Southern Plains—MAM;" "eastern United States—JJA (June–August);" "Northern Plains—SON (September–November);" and "California—ANN." Each region we analyzed contains multiple grid boxes and stations, which reduces the risk of instrumental or reporting errors at a single station controlling results for a given "extreme event." The California region—which in these data did not have annual precipitation anomalies ranked within the lowest three on record during 2013—nonetheless experienced widely publicized drought conditions during 2013, and so is analyzed here.

What is the climate change context for the regional precipitation extremes? Annual or seasonal mean precipitation time series for the focus regions (Fig. 6.1) show some moderate trend-like behavior. For each series, a least squares linear trend (1900–2013) was initially assessed by a standard t test (two-sided; $p = 0.10$), assuming that the residual anomalies, after trend removal, were temporally independent. (This assumption is later relaxed for our model-based assessments.) Three of the regions had significant positive trends (1900–2013): northern tier—ANN; upper Midwest—MAM; and Northern Plains—SON. The eastern United States—JJA had a nonsignificant trend over 1900–2013 but had a significant trend over 1950–2013 (discussed later). The significant trends mentioned above remained significant according to the above preliminary tests even if 2013 was excluded. None of the regions had significant negative trends. Previous studies have noted significant annual mean precipitation increases over much of the central and northern United States (Hartmann et al. 2014), and some increases in flood magnitudes over the north-central United States (Hirsch and Ryberg 2012), although these regional changes were not specifically attributed to anthropogenic forcing.

Observed trends for our selected regions were compared to CMIP5 historical and control runs using a "sliding trend" analysis (Fig. 6.2; Supplementary Fig. S6.3), for a range of start years (all trends ending in 2013), following Knutson et al. (2013a). Sensitivity tests were also performed for trends excluding the

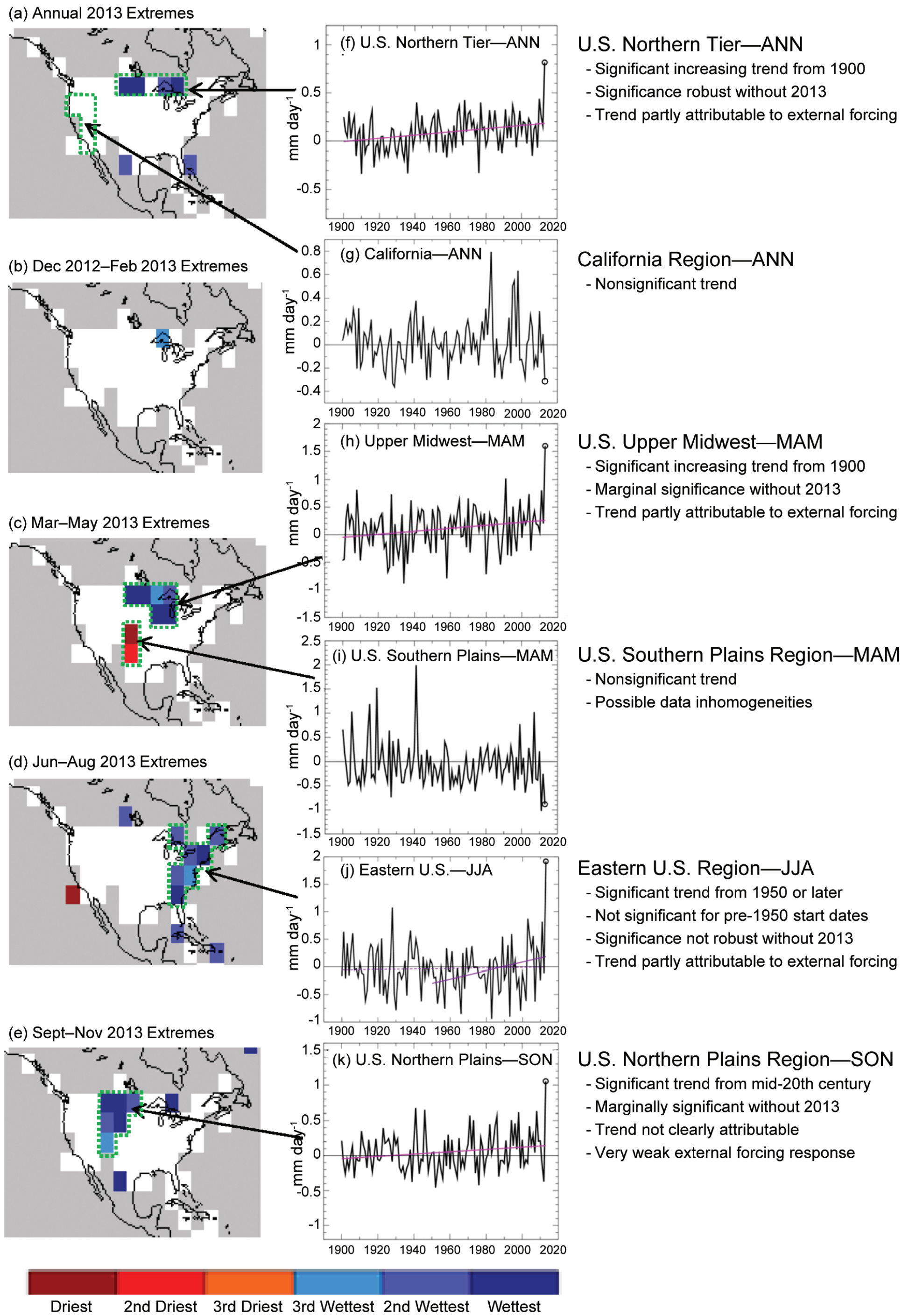

Fig. 6.1. Left column (a–e): Colors identify grid boxes where the annual or seasonal precipitation anomalies for 2013 rank first (dark red), second (red), or third (orange) driest or first (dark blue), second (medium blue) or third (light blue) wettest in the available observed record (see map legend). The seasons are DJF (December 2012–February 2013); MAM (March–May 2013); JJA (June–August 2013); and SON (September–November 2013). The various averaging regions used in the study are shown by the green dashed outlines in (a–e). Gray areas did not have sufficiently long records, defined here as containing at least 100 available annual or seasonal means, with an annual mean requiring at least three of four seasons to be available, and a seasonal mean requiring at least one of three months to be available. Center column (f–k): Time series of precipitation from the extremes regions shown by arrows/green outlines (see also Fig. S6.1 for region definitions). Black: observed anomalies in mm day^{-1}; purple sloping line: significant linear trends (1900–2013, except 1950–2013 for eastern U.S. region—see text for explanation). The observed anomalies for 2013 are circled for emphasis in (f–k). The overall analysis results of the paper are summarized for each region in the right column.

highly anomalous 2013 observed values (Supplementary Fig. S6.3). Briefly, if observed trends were outside of the 5th–95th percentiles of the control run distribution, they were designated as "detectable" compared to internal variability. Detectable positive trends that lie either within or above the 5th–95th percentile range of the All-Forcing (anthropogenic and natural forcing) distribution are interpreted as at least "partly attributable to external forcing." For example, the northern tier—ANN plot (Fig. 6.2b) shows that the positive observed trends in this region are detectable compared to internal variability (black curve outside the purple shading) and at least partly attributable to external forcing (inside the pink shading) for start dates from 1900 to about 1940, but are generally not detectable for trend start dates more recent than 1940.

Figure 6.2e, for the upper Midwest—MAM, indicates detectable trends compared to internal variability, except for mid-20th century start dates. For the eastern United States—JJA (Fig. 6.2h), positive trends are detectable for start years of ~1940 and later but not from the early 20th century. The cases of detectable trends for the three regions discussed above are also generally cases where the observed trends are at least partly attributable to external forcing according to the models (i.e., within or above the pink regions on the "sliding trend" graphs). The robustness of these assessments to exclusion of the highly anomalous 2013 value is examined in Supplementary Fig. S6.3. This analysis indicates that the most robust findings are for the northern tier—ANN region, while the detection result for the recent (late 20th century) trends in the eastern United States—JJA region is not very robust to exclusion of 2013. Intermediate robustness results are indicated for the upper Midwest—MAM region. As discussed in the Discussion section and Supplemental Material, insufficient ensemble sizes for the available CMIP5 Natural Forcing experiments have precluded us from robust trend detection compared to the Natural Forcing-only trend distributions, and so our results do not specifically distinguish a detectable *anthropogenic-only* influence on seasonal/annual precipitation trends for any of the focus regions. Some further discussion of trend results for three additional regions: the Southern Plains—MAM, Northern Plains—SON, and California—ANN is contained in the Supplemental Material.

Are the 2013 regional extremes attributable to anthropogenic and natural forcing? We next examine the 2013 anomalies in particular (relative to 1900–40 baseline values) in the three U.S. regions that had both extreme 2013 anomalies *and* long-term increasing trends that were assessed as partly attributable to anthropogenic and natural forcing: northern tier—ANN, upper Midwest—MAM, and eastern United States—JJA. For each of these regions, the CMIP5 multimodel ensemble-mean of the All-Forcing simulations shows a trend toward increasing rainfall but at a rate much smaller than the observed trend (Fig. 6.2a,d,g; Supplementary Fig. S6.4). Because the modeled response series are noisy for estimating a single-year value (even after ensemble-averaging), we apply temporal smoothing to estimate the 2013 All-Forcing anomaly (Supplementary Fig. S6.4; Supplemental Material). Using this estimated 2013 "All-Forcing" anomaly, we then estimate the 2013 All-Forcing distribution via a "rightward displacement" of the CMIP5 multimodel control run variability distribution (Fig. 6.2c,f,i). Using these forced and unforced anomaly distributions for each region, we estimate the influence of "anthropogenic + natural" forcings on the occurrence rate of extreme anomalies, using the "second-ranked year" anomalies (2010, 1991, or 1928) as the threshold values for fraction of attributable risk (FAR) calculations. We tested using the record 2013 values as the thresholds for FAR calculations but found that those values were either extremely rare or unprecedented in the modeled distributions so that the FAR results were very sensitive to our methodology. Therefore, we report here only the calculations based on the second-ranked years.

Note that the ensemble-mean All-Forcing response (shift between red and blue distributions in Fig. 6.2c,f,i) explains just a small fraction of the observed anomalies for 2013, implying a likely dominant role for internal variability in the 2013 rainfall extremes. For northern tier—ANN, the FAR of threshold-exceeding extremes due to anthropogenic and natural forcing combined is estimated as 0.60, based on estimates using the 2010 observed values as the threshold, with an occurrence ratio (All-Forcing vs. Control runs) of 2.5. In other words, the fraction of current risk of events exceeding the threshold that is attributable to external forcing is about 0.6. For the upper Midwest—MAM region, FAR is estimated as 0.49, with an occurrence ratio of 2.0. For the eastern United States—JJA, the FAR is estimated as 0.36 with an occurrence ratio of 1.6. The FAR estimates discussed here are based on the multimodel ensemble-mean All-Forcing response. However, considerable uncertainty remains in the FAR estimates; for example, FAR estimates based on individual models rather than the multimodel ensemble (not shown) can fall below zero or substantially exceed the multimodel estimates.

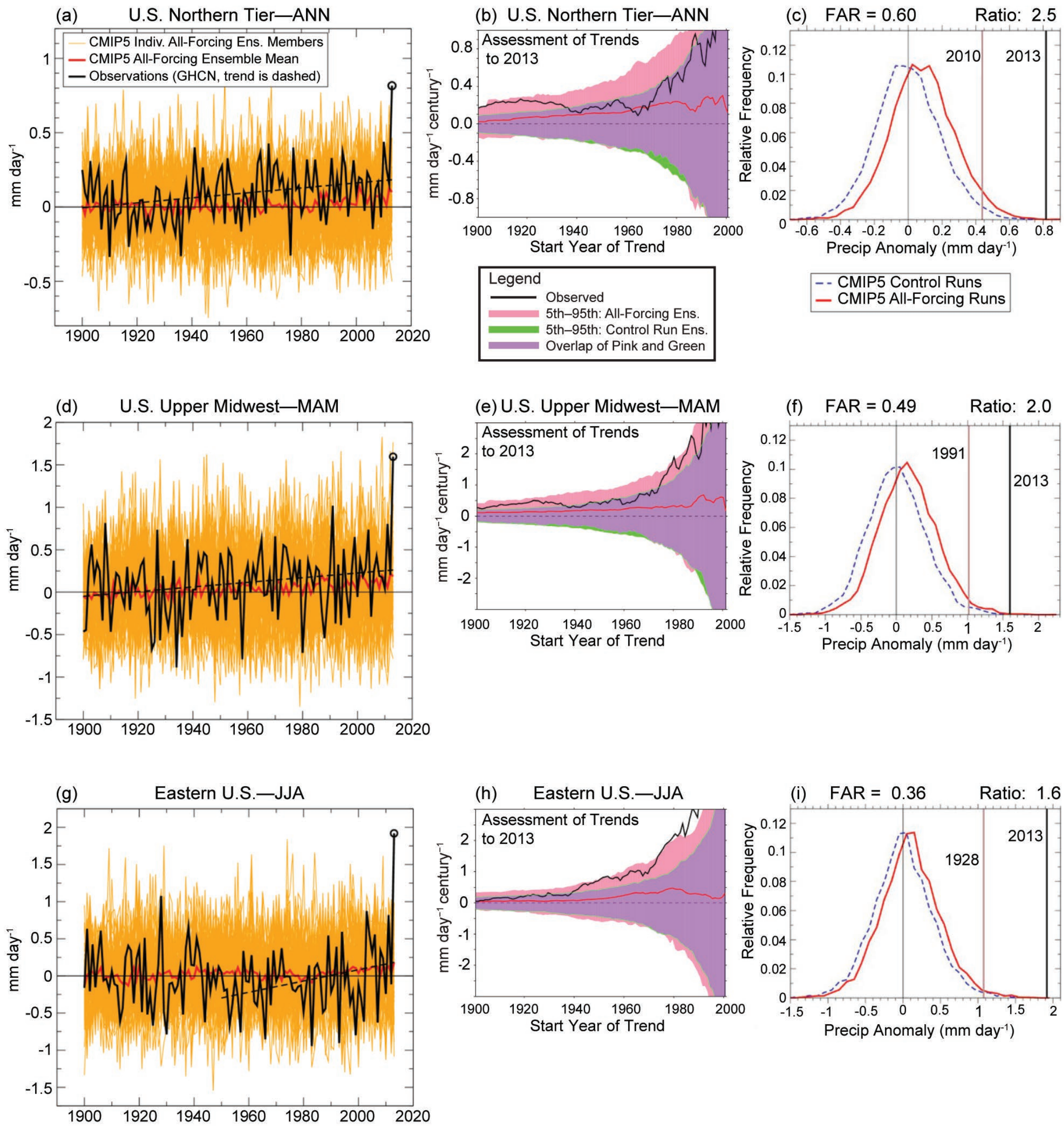

Fig. 6.2. (a,d,g) Rainfall time series averaged over the (a) U.S. northern tier–ANN, (d) U.S. upper Midwest—MAM and (g) eastern U.S.—JJA regions relative to 1900–40 baseline values. Black curves are observations, red curves are CMIP5 ensemble-mean All-Forcing responses, orange curves are individual model ensemble members, and sloping black dashed lines depict significant linear trends for observations. (b,e,h) Sliding trend analysis of precipitation trends for the series in (a,d,g) but for various start years (x-axis) with all trends ending in 2013. Black curves: observed trends; red curves: CMIP5 All-Forcing multimodel ensemble-mean trends; pink shading: 5th–95th percentile range of trends from the CMIP5 All Forcing (anthropogenic + natural forcing) runs, extended to 2013 with RCP4.5 scenarios; green shading: 5th–95th percentile range of internally generated trends from CMIP5 control runs; purple shading: overlap of pink and green regions. (c,f,i) Analysis comparing extreme observed anomalies (relative to 1900–40 baseline) for 2013 or for the next-most extreme year (2010, 1991, 1928) with CMIP5 model-simulated anomaly distributions. Blue histogram: CMIP5 multimodel control run distribution showing model-estimated internal climate variability. Red histogram: All-Forcing distribution obtained by shifting the control run distribution to the right by the estimated All-Forcing ensemble mean response (relative to the 1900–40 baseline) for 2013 (see also Supplemental Material). The black and gray vertical lines in (c,f,i) depict extreme observed anomalies, including the record observed values for 2013 (black) and the second-ranked year (gray), for comparison to the modeled distributions of anomalies. Denoting p_f and p_c as the occurrence rates within the All-Forcing and Control run distributions, respectively, of anomalies exceeding the defined second-ranked-year thresholds shown in the plots, then FAR = $1-p_c/p_f$, and the occurrence ratio is p_f/p_c.

Another important potential source of uncertainty is the adequacy of the control run variability, which is compared to "residual" observed variability in the Supplemental Material (Supplementary Figs. S6.5–7). Our basic findings appear robust to this uncertainty, although the simulation or estimate of internal climate variability remains an important topic for further research.

Discussion and conclusions. Three of the focus regions, northern tier—ANN, upper Midwest—MAM, and eastern United States—JJA, had record or near-record seasonal or annual precipitation anomalies during 2013 as well as detectable positive trends that were at least partly attributable to external forcing (anthropogenic and natural forcing combined). However, detection was marginal for the eastern United States. According to the models, external forcing increased the likelihood of rainfall events as extreme as the observed second-ranked year thresholds by factors of 1.6 to 2.5. The climate change detection here is only with respect to control run (intrinsic) climate variability. We have not attempted detection relative to natural forcing and intrinsic variability combined, since (a) the simulated ensemble-mean response to external forcings is generally much smaller than the observed long-term trends, interannual variability, and 2013 anomalies; and (b) too few simulations with only natural forcing were performed to sufficiently delineate the response to that forcing. Thus, while there is some suggestion of increased risk attributable to anthropogenic forcing in our findings (Supplementary Fig. S6.4), this is not emphasized here due to the lack of a sufficiently detectable long-term anthropogenic trend contribution. Extensions of the CMIP5 Natural Forcing runs through 2013, and larger ensembles of Natural Forcing experiments by various modeling centers, would be particularly useful for further investigations.

Important caveats are that we have not yet systematically analyzed regional precipitation trends globally (which would clarify the large-scale context of our findings), nor have we assessed possible data homogeneity issues, alternative datasets (e.g., Becker et al. 2013), or effects of radiative forcings on precipitation variance. Clearly, it would be much more difficult to detect anthropogenic influences on regional precipitation extremes than on surface temperatures (e.g., Knutson et al. 2013a). This is already evident in other recent analyses of regional precipitation trends (van Oldenborgh et al. 2013; Bhend and Whetton 2013). Nonetheless, some studies have reported detectable anthropogenic influence for zonal-mean precipitation (e.g., Zhang et al. 2007; Marvel and Bonfils 2013), precipitation extremes over large land regions of the Northern Hemisphere (Min et al. 2011), or precipitation changes in the extratropical Southern Hemisphere (Fyfe et al. 2012) or Mediterranean region (Hoerling et al. 2012). We conclude that the 2013 extreme precipitation "events" for three U.S. regions/seasons (northern tier—ANN, upper Midwest—MAM, and eastern United States—JJA) are tentatively attributable in part to external (anthropogenic and natural) forcing, with a likely much larger additional contribution from unforced intrinsic variability. We suggest that these regions be monitored for possible future emergence of anthropogenically forced precipitation increases, including more extreme seasonal or annual mean rainfall.

7. OCTOBER 2013 BLIZZARD IN WESTERN SOUTH DAKOTA

Laura M. Edwards, Matthew J. Bunkers, John T. Abatzoglou,
Dennis P. Todey, and Lauren E. Parker

An early October blizzard in South Dakota is determined to be climatologically anomalous. Climate models suggest that early autumn extreme snowfall events in western South Dakota are less likely due to anthropogenic climate change.

Introduction. An early season blizzard on 4–5 October 2013 in western South Dakota (SD) and neighboring areas of Wyoming, Nebraska, and North Dakota caused severe infrastructure damage and economic losses to businesses and agricultural communities. Estimated losses total $38 million in SD alone.

The blizzard produced 50.8–99.6 cm of snow across the plains and 139.7 cm of snow in the northern

SUPPLEMENT

EXPLAINING EXTREME EVENTS OF 2013 FROM A CLIMATE PERSPECTIVE

Editors
Stephanie C. Herring, Martin P. Hoerling, Thomas C. Peterson, Peter A. Stott,

Special Supplement to the
Bulletin of the American Meteorological Society
Vol. 95, No. 9, September 2014

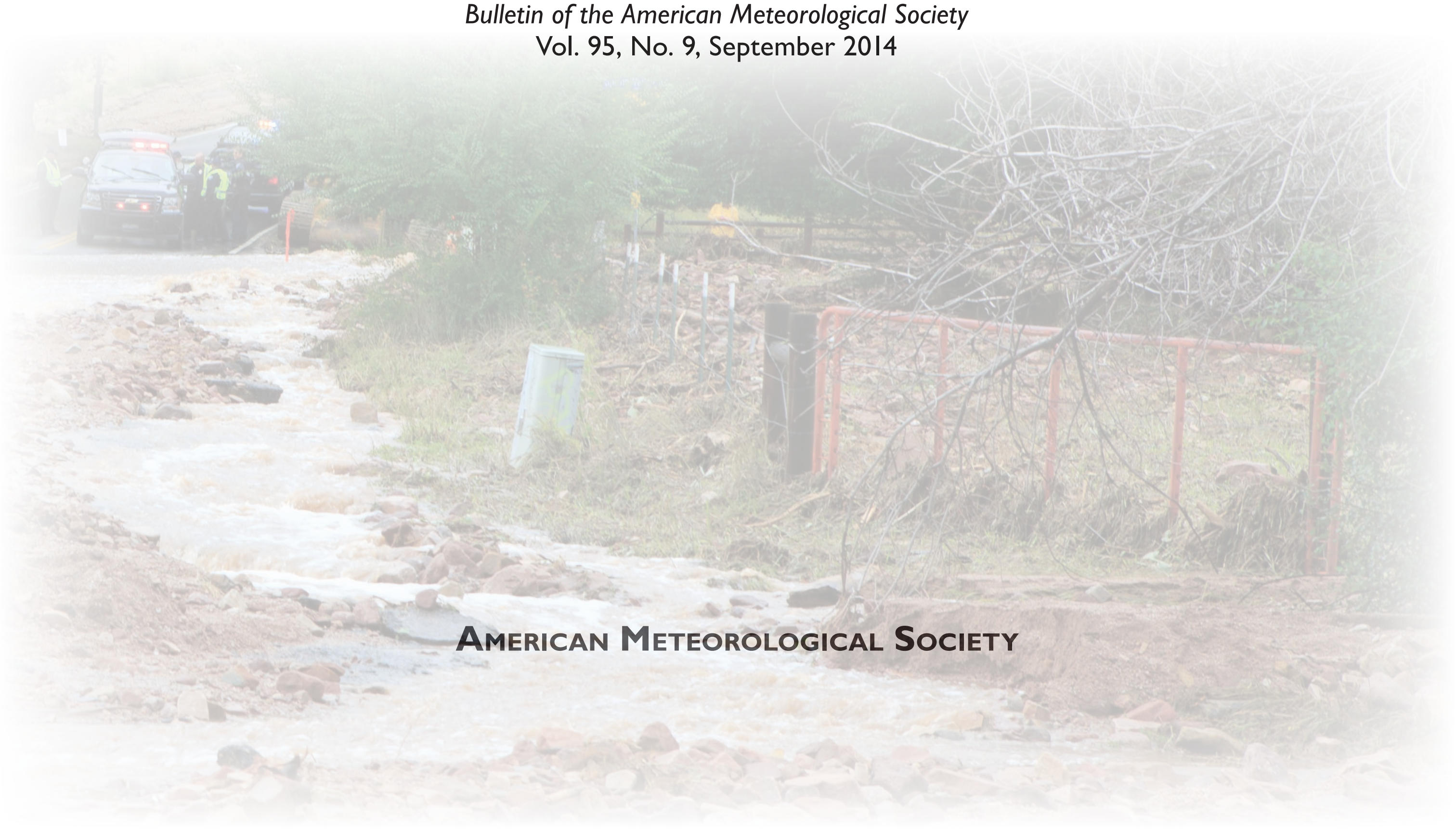

AMERICAN METEOROLOGICAL SOCIETY

S6. SEASONAL AND ANNUAL MEAN PRECIPITATION EXTREMES OCCURRING DURING 2013: A U.S. FOCUSED ANALYSIS

Thomas R. Knutson, Fanrong Zeng, and Andrew T. Wittenberg

In this supplemental material, we provide additional background, discussion, and analysis, including: region definitions, global precipitation anomaly maps, and locations with extremes in 2013; areal coverage of record or near-record anomalies by year; spatial resolution issues for observed data; additional sliding trend analysis and sensitivity tests; a description of methodology for estimating the 2013 multimodel ensemble All-Forcing anomaly and the fraction of attributable risk (FAR); and an assessment of model-simulated precipitation and internal variability. Table S6.1 provides a list of the Coupled Model Intercomparison Project phase 5 (CMIP5) models used in the study.

Region definitions, global anomaly maps, and locations with seasonal/annual extremes in 2013. Figure S6.1 shows global maps of (a–e, left column) annual and seasonal mean precipitation anomalies for 2013 and (f–j, middle column) the grid locations with record or near-record wet or dry conditions (seasonal or annual mean precipitation ranked first, second, or third highest or lowest in the available record of length at least 100 years). The blue regions in the right column outline the focus regions selected for the study based on their 2013 anomalies. The six focus regions, including the designated name and season or annual mean, are the northern tier region of states along the northern U.S./Canadian border region with extreme positive annual-mean anomalies ("northern tier—ANN"); in March–May (MAM) a similar region of the northern United States extending slightly further south, also with extreme positive anomalies ("upper Midwest—MAM"); during MAM, a region of record or near-record low precipitation occurring over the southern U.S. Plains ("Southern Plains—MAM"); in Northern Hemisphere (NH) summer (June–August, JJA), extreme positive anomalies occurring over regions of the eastern United States ("eastern U.S.—JJA"); and in NH fall (September–November, SON), extreme positive anomalies occurring in a region of the north-central United States, but slightly to the west of our upper Midwest region ("Northern Plains—SON"). Although the California region, as resolved in the Global Historical Climatology Network (GHCN) gridded data, was not identified in our analysis as having extreme seasonal or annual precipitation in 2013 (i.e., ranked within the lowest three on record), because of notable drought conditions occurring there during 2013, we examined annual precipitation anomalies in this region ("California—ANN") as well as seasonal anomalies for December 2012–February 2013 (DJF) and MAM 2013.

Percent coverage of extreme annual mean wet and dry anomalies by year (1900–2013). The extremes maps, Fig. S.6.1 (f–j) show that the high and low mean precipitation extremes were well dispersed around the globe during 2013. Figure S6.2 shows that about 2% of the global "available data" area experienced annual mean dry extremes (first, second, or third lowest rainfall) in 2013, while about 5% experienced wet annual mean extremes (first, second, or third highest rainfall). Since extremes are expected to occur in some places around the globe in any given year, an interesting question is whether 2013 is unusual in terms of the percent area with extreme annual mean values. As a preliminary analysis of this issue, we show in Fig. S6.2 the time series of the fraction of area with wet and dry annual mean extremes over

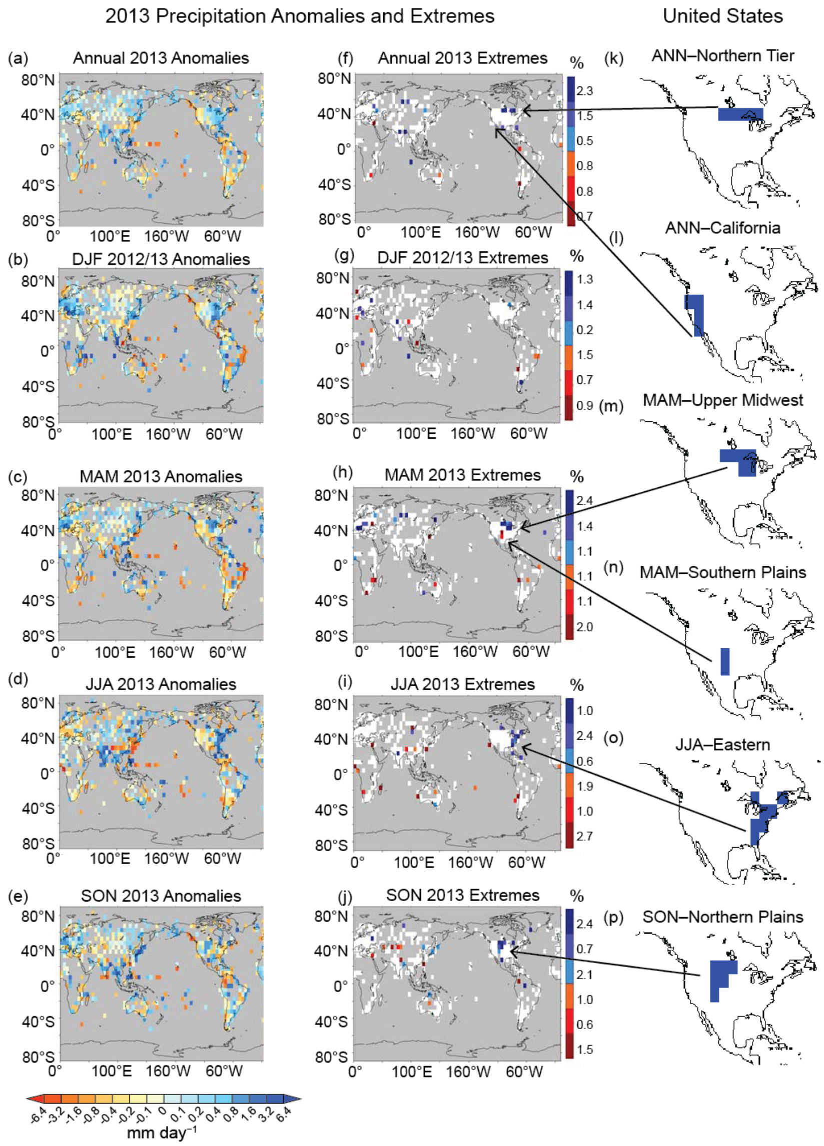

Fig. S6.1. Left column: precipitation anomalies for 2013 (annual or seasonal) in mm day^{-1}. The middle column panels indicate where the anomalies for 2013 are ranked 1st, 2nd, or 3rd wettest or driest in the available record of at least 100 years in length (see Fig. 6.1 legend in the main report). Dark, medium, and light blue depict grid boxes where the 2013 seasonal or annual means rank 1st, 2nd, or 3rd wettest on record. Dark red, red, and orange are 1st, 2nd, and 3rd driest on record. Percent values alongside the color bar in the middle-column panels indicate the percent of global available area with the indicated category of 2013 extreme – where the "available area" has adequate data coverage for at least 100 years (Fig. 6.1 caption in the main report). The blue regions in the right column depict the domains of the six U.S. focus regions selected for our study based on their 2013 extreme anomalies.

the entire record (1900–2013). We include two different measures: (a) the fraction of area with top-three or bottom-three ranked values for each year using the data up to that year and (b) the fraction that is ranked top-three or bottom-three using all years that are eventually available in the series (1900–2013). These metrics show that there has been a tendency for a larger areal coverage of wet annual mean extremes versus dry extremes in recent decades, and particularly since about 1990. The time series suggest a possible emerging trend in prevalence of wet annual mean precipitation extremes over dry annual extremes. However, the assessment of whether there is a significant trend in these measures is a nontrivial

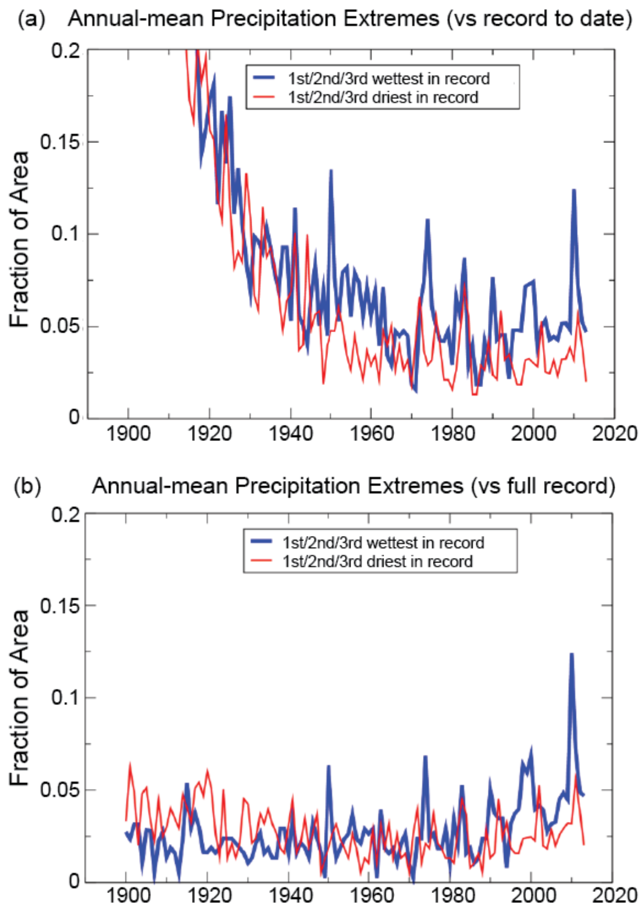

Fig. S6.2. Time series show the fraction of global available area each year with annual mean precipitation anomalies that are ranked 1st through 3rd wettest (blue line) or driest (red line) for each year from 1900 to 2013. The rankings in (a) are based on the available data to date for each particular year (which means that occurrences of new records and near-records are very common in the earlier years). Rankings for (b) are based on the full available record, including years that come after the year in question. This removes the "early year" bias of the method shown in (a).

task. For example, Livezey and Chen (1983) describe issues associated with global significance of areal coverage of locally significant results. Christiansen (2013) addresses the problem of the significance of numbers of record occurrences of warm temperatures and finds that trends in warm daily records for the Northern Hemisphere extratropics since the 1940s are very statistically significant, while trends in monthly warm records are not significant. An assessment of whether the trend suggested in Fig. S6.2 represents a significant change or whether 2013 is a "special" year in any sense in terms of global coverage is beyond the scope of the present study but will be the subject of future investigation.

Resolution dependence (observed data). Owing to the coarse grid on which the data are available, we examine only a very spatially smoothed precipitation anomaly—though the grids are similar to the grid scales of the climate models. Preliminary analysis of an alternative much higher resolution global gridded precipitation dataset (Becker et al. 2013) not only confirms the general occurrence of extreme precipitation anomalies during 2013 in the regions that we focus on, but it also indicates that the record or near-record seasonal anomalies are typically concentrated within relatively small subregions compared to the grid boxes depicted in Fig. S6.1. A separate analysis of about 60 individual U.S. stations in the northern tier region reveals that eight of these stations had unprecedented annual anomalies in 2013 (Cody Hewitt, Rutgers University, 2014, personal communication). Daily timeseries at these eight stations indicate that the unusual annual totals were typically comprised of several large precipitation events, typically occurring in the spring, summer, or autumn.

Sliding trend analysis for all focus regions and sensitivity to excluding 2013 data. Figure S6.3 shows the sliding trend analysis (All-Forcing runs versus Control runs) for each of the six focus regions. Note that the reason we use control runs in our analysis to create the distributions of trends and of variability for the All-Forcing cases (e.g., Fig. 6.2 in the main report and Fig. S6.3) is that the CMIP5 archive does not contain enough individual All-Forcing ensemble members to sample the internal variability of the individual models adequately for various start dates. Therefore, we have chosen to use samples of variability from the control runs to estimate the range of possible trends around the mean estimates provided by the CMIP5 individual model All-Forcing runs. The All-Forcing 5th to 95th percentile range in Fig. 6.2 in the main report and Fig. S6.3 is based on the aggregate distribution of All Forcing trends and includes a spread due to both differences in ensemble mean response of the various individual models as well as intrinsic (control run) variability, with all control runs sampled equally frequently (see Knutson et al. 2013 for further methods details).

Figure S6.3 (middle column) shows the sliding trend analysis for trends extending to 2013, while the

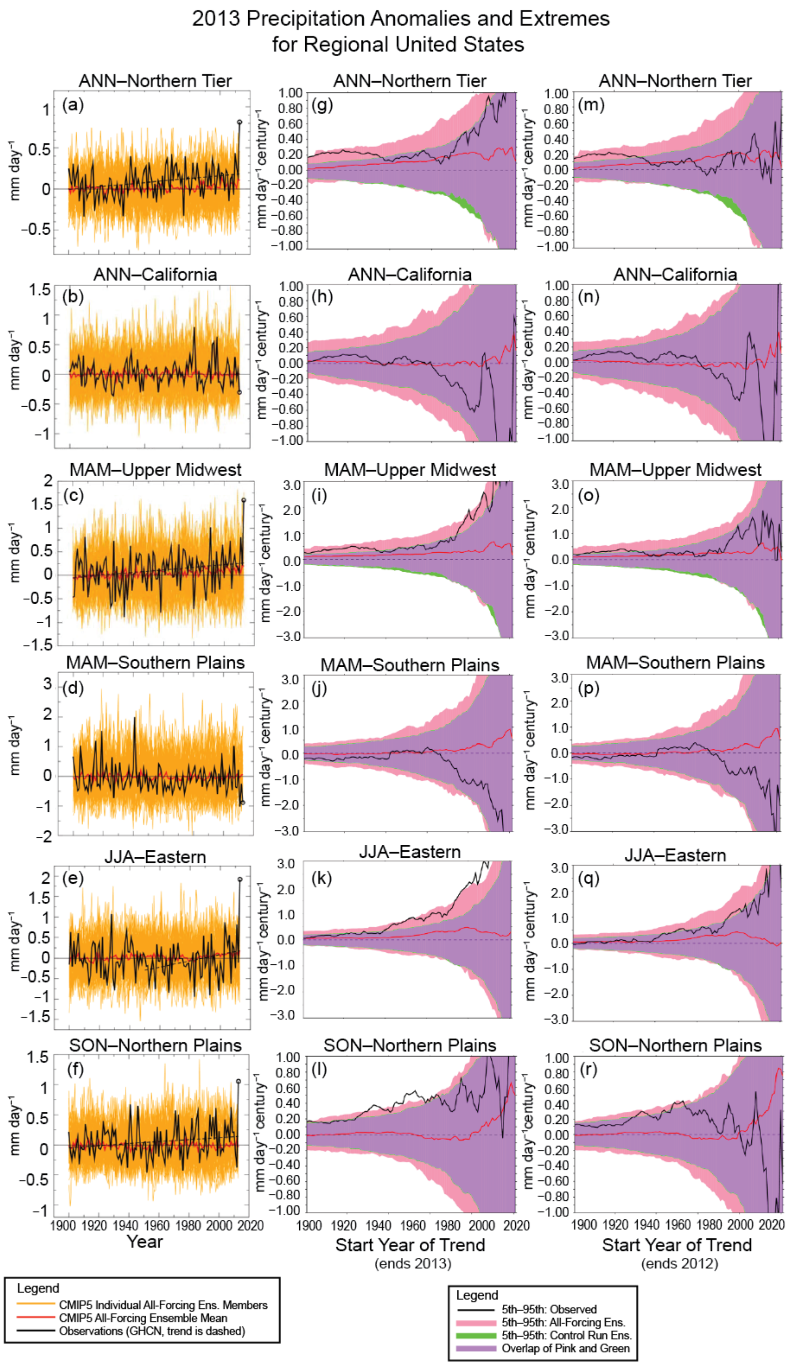

Fig. S6.3. Left (a–f) column shows time series for each of six regions and is analogous to the left column of Fig. 6.2 in the main report. The center (g–l) column is as in Fig. 6.2 in the main report, but shows the sliding trend analysis for each of the six focus regions for trends to 2013. The right column (m–r) analyzes trends for the same regions but excludes 2013 as a sensitivity test. See Fig. 6.2 in the main report caption and text for further details.

right-hand column shows trends to 2012, to test the effect of leaving out the highly anomalous end year (2013). While excluding 2013 has only a minor impact on the detection results for the northern tier—ANN region Fig. S6.3 (g,m) for trends starting prior to 1930, it has a major impact on the late 20th century trend detection results for the eastern U.S.—JJA region Fig.6.3 (k,q). The latter detection result is not robust to excluding 2013 and thus depends quite critically on the one highly unusual year. Results for the upper Midwest—MAM are intermediate between these results; leaving out 2013 substantially reduces the robustness of the trend detection, but the trends from the early 20th century to 2012 are still generally detectable according to the models.

We now discuss the three remaining U.S. regions from Fig. 6.1 in the main report, which were not discussed in detail in the main text (California—ANN, Southern Plains—MAM, and Northern Plains—SON). Two of these regions did not exhibit significant linear trends according to statistical tests on linear trends over 1900–2013 (California—ANN and Southern Plains—MAM). These regions also do not have detectable long-term trends according to the model-based trend detection tests shown in Fig. S6.3 (h,j). California region trends were also not detectable for the DJF or MAM seasons (not shown). The U.S. Northern Plains—SON region analysis (Fig. S6.3l) indicates some detectable trends to 2013 (All-Forcing runs versus Control runs). Trends to 2013 are detectable beginning in the 1930s, 40s, and 50s, as shown by the black line extending above the purple shaded region. However, for this region the All-Forcing ensemble mean response (red line) is relatively small or even negative, except for trends beginning quite late in the 20th century, at which point the observed trends are not detectable. Note that the pink shaded region (5th to 95th percentile of All-Forcing trends) is slightly broader than the control run trend distribution but is also centered around the purple (control run overlap) shading, in contrast to the positive skewing of the pink shaded region compared to the purple shading for the other regions in Fig.S6.3. This lack of positive skewing of the All-Forcing shaded region compared to the control is also indicative of the very weak All-Forcing response in the models for this region. The broadening of the pink region relative to the green/purple region is due to the former runs having a diversity of model responses to external forcings, while the latter runs had unchanging preindustrial forcings. The very small CMIP5 century-scale ensemble mean All-Forcing responses (red line) in the Northern Plains—SON region suggest that internal variability is the dominant contributor to the observed long-term trends in this region. This finding assumes that the All-Forcing response is adequately modeled by the CMIP5 models. Finally, our sensitivity tests excluding 2013 (Fig. S6.3r) indicate that the Northern Plains—SON region trend detection results are not very robust to the exclusion of 2013.

The Southern Plains—MAM region time series exhibits some additional interesting behavior. The time series (Fig. S6.3d) shows several decades with very pronounced variations prior to about 1945, followed by several decades with much smaller variability. Although we find no detectable trends in this region, we suggest that the observed dataset here may require further assessment for possible temporal inhomogeneities, perhaps associated with secular changes in the observing network.

Although not shown here, we also performed some sliding trend analysis comparing the observed trends to CMIP5 Natural Forcing-only distributions. However, we had difficulties with this analysis owing to the relatively few models with available Natural Forcing runs extending to 2012, the relatively small number of ensemble members (in some cases, only one) for the available models, and the relatively few distinct modeling centers that have provided such runs so far. For these reasons, we are not presenting results from the All-Forcing versus Natural Forcing sliding trend analysis in this study.

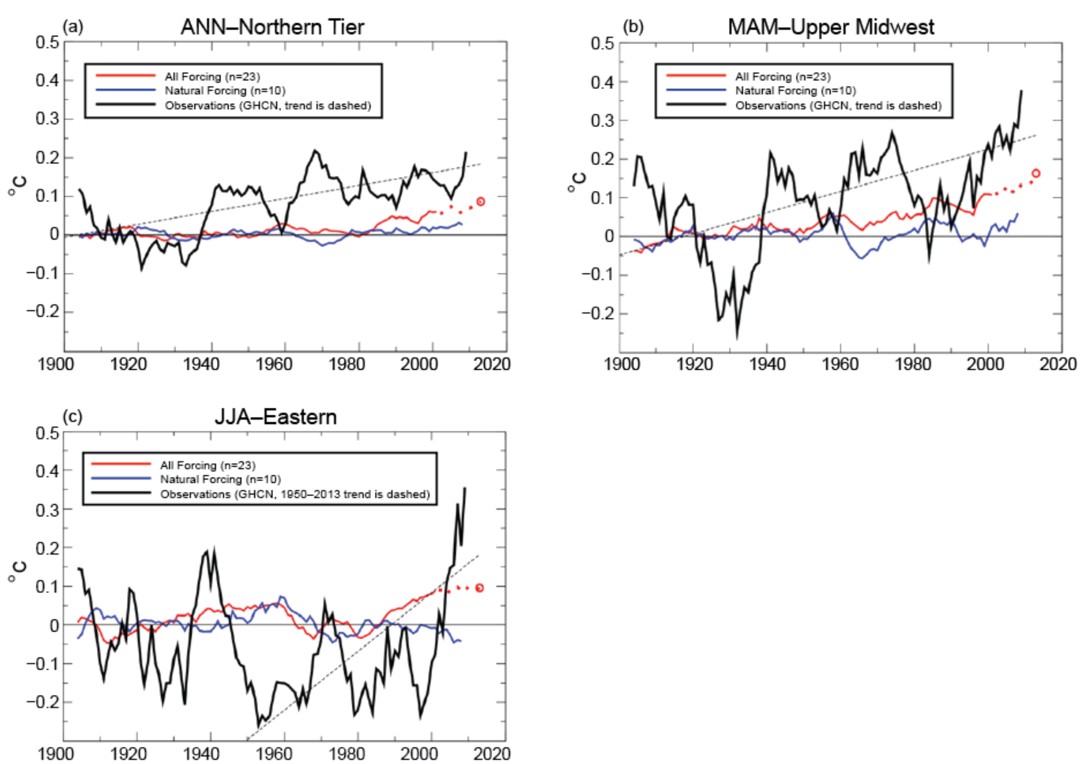

Fig. S6.4. CMIP5 multimodel ensemble mean All-Forcing (red) or Natural Forcing-only (blue) 9-yr running-mean anomalies relative to a 1900-1940 baseline. Time series shown are based on annual (a), March–May (b), or June–August (c) averaged data. Observed 9-yr running means are shown by the black thick lines in each diagram, with the linear trends of annual means shown by the black dashed lines. Results are shown for a) northern tier-ANN, b) upper Midwest—MAM, and c) eastern U.S.—JJA regions/seasons. The red circles at year 2013 show the 9-yr running mean All-Forcing anomaly centered on 2013. All-Forcing ensemble time series values that include any years beyond 2005 (and thus include some RCP4.5 projection values for at least some models) are denoted by the red-dashed segments. See text for further details.

Methodology for estimating the 2013 multimodel ensemble All-Forcing anomaly and the FAR. The time series (Fig. 6.2 a,d,g in the main report) depict the CMIP5 multimodel All-Forcing ensemble mean, relative to the 1900–40 baseline, as a dark red line; the upward-sloping black-dashed lines depict the observed linear trends from 1900 to 2013 (or 1950–2013 for Fig. 6.2g in the main report). The All-Forcing response is small and difficult to see in Fig. 6.2 in the main report, so it is shown in an expanded view (with nine-year running mean smoothing) for each region in Fig. S6.4 (thin red lines). Note that the All-Forcing ensemble mean responses are much smaller than the observed nine-year running mean changes and smaller than the observed linear trends (dashed black lines). The ensemble mean has considerable year-to-year variation (Fig. 6.2 a,d,g in the main report), so estimating the All-Forcing model ensemble's mean for the year 2013 is difficult. Our approach is to estimate the 2013 value by using a temporally smoothed (nine-year running mean) version of the ensemble mean time series. To obtain a nine-year running mean value centered on 2013, we extended the All-Forcing response curves to 2017 using the RCP4.5 scenarios in the model archives. The smoothed 2013 All-Forcing values (red circles in Fig. S6.4) are then used to shift the control run distributions in Fig. 6.2c,f,i in the main report to create the All Forcing distributions for 2013 shown in Fig. 6.2c,f,i in the main report and used for our FAR analysis. The red curves in Fig. S6.4 are dashed for values from 2001 on to indicate that these values are at least partly influenced by the RCP4.5 extensions beyond 2005 in the model data.

The blue curves in Fig. S6.4 show the Natural Forcing-only ensemble (10-model) results analogous to those for the All-Forcing ensemble just discussed. In principle, these could be used to create "Natural Forcing-only" versions of the distributions in Fig. 6.2c,f,i in the main report from which a fraction of attributable risk to anthropogenic forcing could be estimated. We have chosen not to do this, however, because of the lack of a long-term detectable trend in

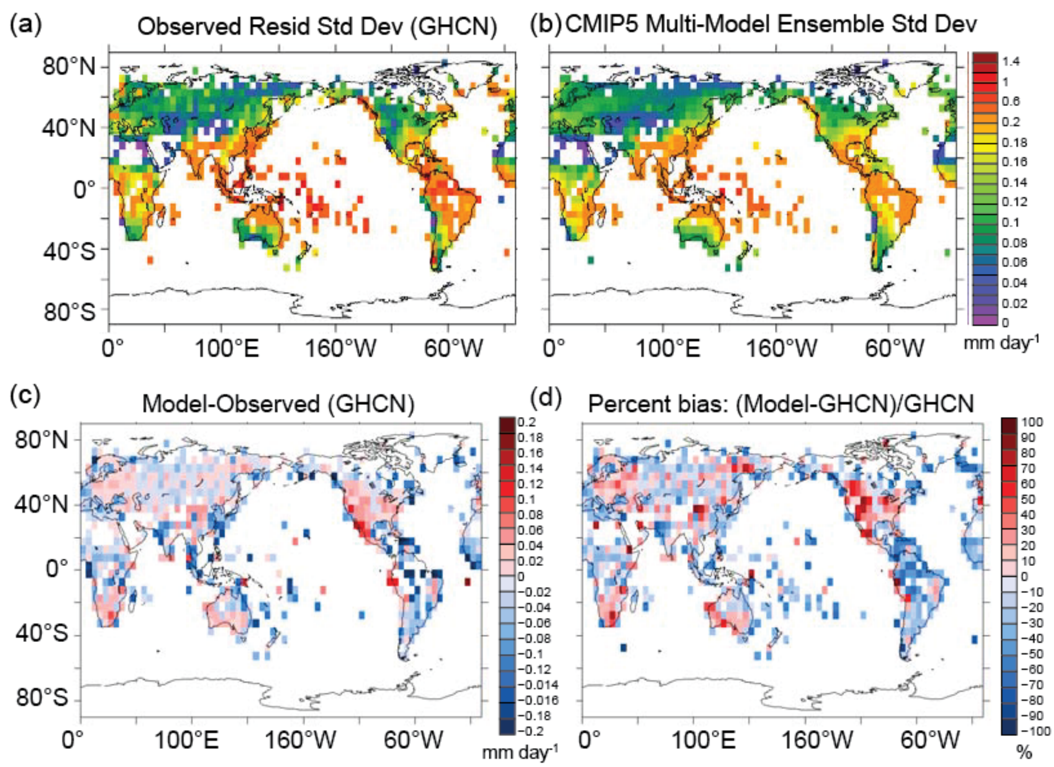

Fig. S6.5. Maps of standard deviation of low-pass (>10 yr filtered) precipitation anomalies (mm day^{-1}) based on annual data for: (a) GHCN observed residuals (1900–2013); and (b) the ensemble-mean standard deviation from the 23 CMIP5 control runs used in this study. The observed residuals were formed by subtracting the CMIP5 multi-model ensemble All-Forcing/RCP4.5 response from the observations to create annual mean residual anomalies series for comparison with the control run (intrinsic variability) simulations. (c) Bias map computed as the modelled standard deviation in (b) minus the observed residuals standard deviation in (a). (d) Same as in (c) but expressed as percent bias: [(model – observation)/observation] × 100%.

these focus regions compared to the Natural Forcing-only distributions, as discussed previously.

FAR is the fraction of attributable risk for anomalies as large as certain threshold values (here we use the second-ranked year in the observed record), and it is based on the All-Forcing anomaly distributions for 2013 compared to the unforced anomaly distributions. In this case, the fraction of risk is attributable to anthropogenic and natural forcing combined. The occurrence ratio (All-Forcing : Control) is the occurrence rate of anomalies as large as those for the second-ranked year under the All-Forcing scenario, divided by the corresponding rate in the control run distribution. FAR and the occurrence ratio are computed as follows: FAR = 1–pc/pf, and the occurrence ratio is pf/pc, where pf and pc are the occurrence rates within the All-Forcing and Control run distributions, respectively, of anomalies exceeding the defined thresholds shown in the plots (thick gray vertical lines) in Fig. 6.2c,f,i in the main report.

Assessment of model-simulated precipitation and internal variability. How adequate are the CMIP5 models' simulations of precipitation in the focus regions? Of particular interest is the climate variability in their control runs, which we have used to estimate the real world's intrinsic (unforced) climate variability. For the CMIP5 models, an assessment of the ensemble-mean precipitation geographical distribution and seasonal cycle was done by Flato et al. (2013; see Figs. 9.4, 9.38, 9.39 in the main report). Despite model biases, their figures suggest that the CMIP5 simulations of large-scale precipitation characteristics in our focus regions are sufficiently realistic for our purposes.

Examining variability, Fig. S6.5 shows the geographical distribution of low-frequency (>10 years) (standard deviations of annual precipitation for the observations (GHCN) versus the CMIP5 multimodel ensemble standard deviations from the model control runs. To make the observed standard deviations more comparable to control runs (which represent intrinsic climate variability alone) we subtracted the multimodel mean All-Forcing response from the observed time series to create a residual intrinsic variability estimate, which was then smoothed to include primarily variability with time scales longer than 10 years. The comparison shows (Fig. S6.5) that the models' standard deviation typically exceeds the observed low-frequency standard deviation in the U.S. regions where we are focusing. So, for our trend detection, the models may overestimate the intrinsic variability (i.e., the width of the green/pink/purple bands in Fig. 6.2 b,e,h in the main report and the widths of the distributions in Fig. 6.2 c,f,i in the

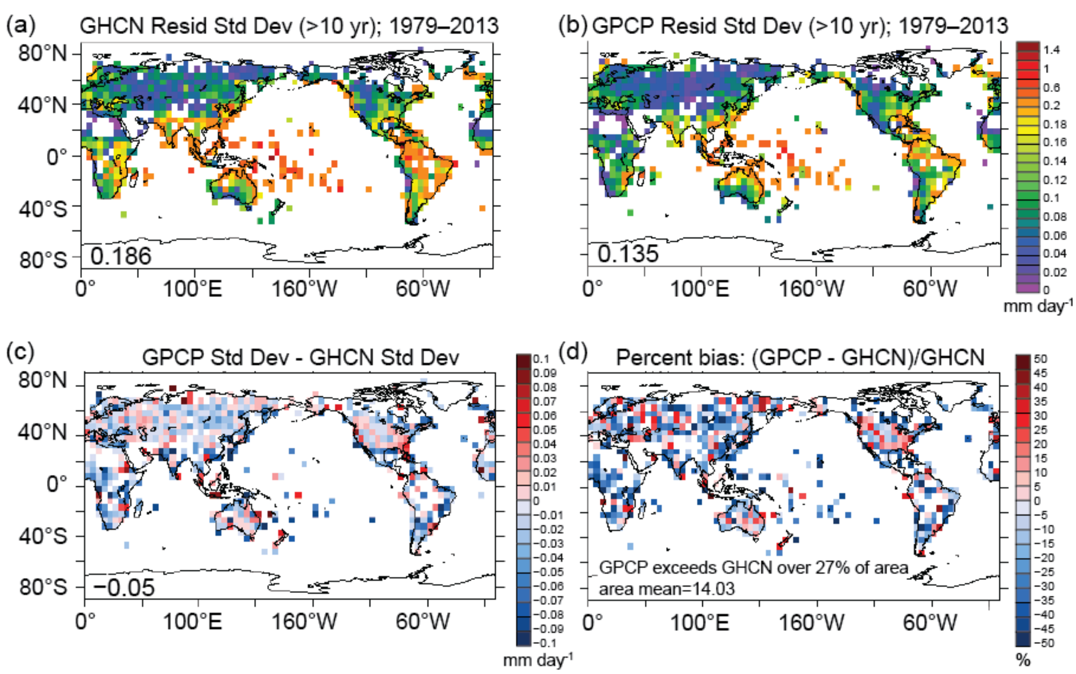

Fig. S6.6. As in Fig. S6.5, but comparing the >10 yr standard deviations of two different observational datasets for the shorter period (1979–2013). The two observational data sets are: (a) GHCN as in Fig. S5a, and (b) GPCP v2.2 (see text for details). (c) and (d) are difference maps and percent difference maps, respectively, for GHCN vs. GPCP. Note the different scales used for Figs. S6.5 vs. S6.6 for panels (c) and (d).

main report). Figure S6.6 also compares the observed GHCN low-frequency (> 10 years) standard deviation for the period 1979–2013 to that of an alternative (combined satellite/rain gauge) dataset over the area of common coverage (Global Precipitation Climatology Project v. 2.2; Adler et al. 2003; http://www.esrl.noaa.gov/psd/data/gridded/data.gpcp.html). This shows that there are even substantial uncertainties in estimating the precipitation standard deviations from observations, which is an important further caveat to our analysis and assessment. Also, comparison of the GHCN standard deviation for the short (1979–2013) versus full (1900–2013) data period (Fig. S6.5 versus Fig. S6.6) shows that the standard deviation is considerably larger for the full period, especially over the Northern Hemisphere continents, which illustrates the impact of the epoch considered for the decadal variability in the GHCN data.

The models' high-frequency (unfiltered annual means) intrinsic variability is also used in our study for the FAR analysis. Therefore, we also need to assess the models' high-frequency variability. To assess this issue, we performed the following auxiliary calculations. For each of the three key regions where we found a detectable trend (northern tier—ANN, upper Midwest—MAM, and eastern U.S.—JJA) we compute an observed residual variability series by subtracting the multimodel ensemble mean All-Forcing response from the observed series. We remove the mean of these residuals and compare their histogram to that from the multimodel control run ensemble, which was obtained by combining 1000-member random samples from each of the 23 CMIP5 control runs into a 23 000 member aggregate control run distribution. The comparison of modeled and observed distributions for each region (Fig. S6.7) indicates that the multimodel ensemble provides a fairly realistic distribution of intrinsic variability, compared to the observed residual distribution. The standard deviations of the control run distributions for the northern tier—ANN and upper Midwest—MAM series are close to but slightly larger (8% and 4%, respectively) than the standard deviation of the observed residual series. This suggests that the mod-

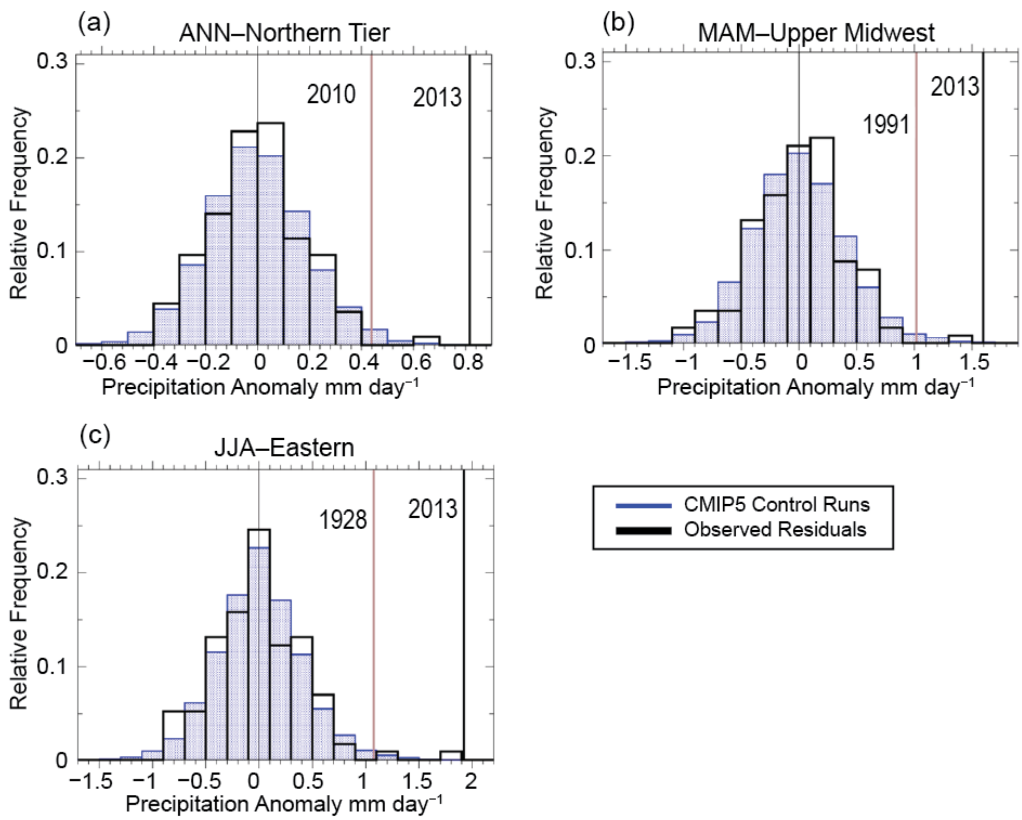

Fig. S6.7. Normalized histograms of annual- or seasonal-mean anomalies from the 23 CMIP5 model control runs (blue bars) vs. observed (GHCN) residuals (black bars). The observed residuals are computed by subtracting the CMIP5 All-Forcing ensemble mean response from the observed time series, and also subtracting the mean of these residuals (resulting in residuals having zero mean). Observed values for 2013 and the alternative threshold value are depicted by the thick black and gray vertical lines (see year labels).

eled estimates are likely adequate for our climate change detection purposes, although they will tend to make it slightly harder to detect forced trends and easier for the All-Forcing estimates to encompass the observations. For the eastern U.S.—JJA region, the observed residual standard deviation is slightly larger (8%) than for the model control runs. Therefore, as a sensitivity test, we amplified the control run anoma-

Table S6.1. Lists of CMIP5 models used in the study for All Forcing (top) and Natural-Only Forcing (bottom) experiments. The lists include the short names of the models, the number of ensemble members included in our analysis in [ ]'s, and a longer name for the modeling center.

All-Forcing Experiments:
BCC-CSM1.1 [3] Beijing Climate Center
CanESM2 [5] Canadian Centre for Climate Modelling and Analysis
CCSM4.0 [6] National Center for Atmospheric Research (U.S.)
CMCC-CM [1] Centro Euro-Mediterraneo per i Cambiamenti Climatici (Italy)
CNRM-CM5 [1] Centre National de Recherches Meteorologiques (France)
CSIRO Mk3.6.0 [1] Commonwealth Scientific and Industrial Research Organisation (Australia)
FGOALS-g2 [5] State Key Lab. Numerical Modeling for Atmos. Sci. and Geophys. Fluid Dyn. (China)
GFDL CM3 [5] Geophysical Fluid Dynamics Laboratory (U.S.)
GFDL-ESM2M [1] Geophysical Fluid Dynamics Laboratory
GFDL-ESM2G [1] Geophysical Fluid Dynamics Laboratory
HadGEM2-ES [4] Hadley Centre (United Kingdom)
INM-CM4 [1] Institute of Numerical Mathematics (Russia)
IPSL-CM5B-LR [1] L'Institut Pierre-Simon Laplace (France)
IPSL-CM5A-MR [3] L'Institut Pierre-Simon Laplace
IPSL-CM5A-LR [6] L'Institut Pierre-Simon Laplace
MIROC5 [5] Model for Interdisciplinary Research on Climate (Japan)
MIROC-ESM [3] Model for Interdisciplinary Research on Climate, Earth System Model
MIROC-ESM-CHEM [1] Model for Interdiscipl. Res. on Climate, Earth Sys. Mod, Chemistry Coupled
MPI-ESM-MR [3] Max Planck Institute (Germany)
MPI-ESM-LR [3] Max Planck Institute
MRI-CGCM3 [3] Meteorological Research Institute (Japan)
NorESM1-M [3] Norwegian Earth System Model
NorESM1-ME [1] Norwegian Earth System Model
Natural-Only Forcing Experiments:
BCC-CSM1.1 [1] Beijing Climate Center
CanESM2 [5] Canadian Centre for Climate Modelling and Analysis
CNRM-CM5 [1] Centre National de Recherches Meteorologiques (France)
CSIRO Mk3.6.0 [5] Commonwealth Scientific and Industrial Research Organisation (Australia)
GISS-E2-H [5] Goddard Institute for Space Studies (U.S.)
GISS-E2-R [5] Goddard Institute for Space Studies (U.S.)
HadGEM2-ES [1] Hadley Centre (United Kingdom)
IPSL-CM5A-MR [3] L'Institut Pierre-Simon Laplace (France)
IPSL-CM5A-LR [3] L'Institut Pierre-Simon Laplace
NorESM1-M [1] Norwegian Earth System Model

lies for this region by a factor of 1.08 and found that this had only a modest impact on our FAR or occurrence ratio estimates in Fig. 6.2i in the main report since this adjustment affects both the control and All-Forcing distribution similarly. The FAR estimate was 0.36 for the unadjusted anomalies versus 0.26 for the amplified anomalies. For the FAR estimates, we used 4000-member random samples from each model for a total sample size of 92 000. Also, the detection results shown for the eastern U.S.—JJA in Fig. 6.2f in the main report are robust to an order 8% increase in the 95th percentile of the control run trends, but as mentioned previously, the trend detection results for this region are sensitive to the inclusion/exclusion of 2013 observed values.

In summary, our variability assessments suggest that the CMIP5 models can provide a useful assessment of precipitation low-frequency variability (trends) and annual or seasonal anomalies due to intrinsic climate variability. This provides support for using these models for our trend assessments and FAR calculations.

REFERENCES

Adler, R. F., and Coauthors, 2003: The Version 2 Global Precipitation Climatology Project (GPCP) monthly precipitation analysis (1979-Present). *J. Hydrometeor.*, **4**, 1147–1167.

Alexandersson, H., T. Schmith, K. Iden, and H. Tuomenvirta, 1998: Long-term variations of the storm climate over NW Europe. *Global Atmos. Ocean Sys.*, **6**, 97–120.

——, H. Tuomenvirta, T. Schmith, and K. Iden, 2000: Trends of storms in NW Europe derived from an updated pressure data set. *Climate Res.*, **14**, 71–73.

Allan, R., and C. K. Folland, 2012: [Global climate] Atmospheric circulation: Mean sea level pressure [in "State of the Climate 2011"]. *Bull. Amer. Meteor. Soc.*, **93** (7), S35–S36.

——, and B. J. Soden, 2008: Atmospheric warming and the amplification of precipitation extremes. *Science*, **321**, 1484.

Allen, M., 1999: Do-it-yourself climate prediction. *Nature*, **401**, 642.

——, 2003: Liability for climate change. *Nature*, **421**, 891–892.

Andermann, C., L. Longuevergne, S. Bonnet, A. Crave, P. Davy, and R. Gloaguen, 2012: Impact of transient groundwater storage on the discharge of Himalayan rivers. *Nature Geosci.*, **5**, 127–132.

Arblaster, J. M., and L. V. Alexander, 2012: The impact of the El Niño-Southern Oscillation on maximum temperature extremes. *Geophys. Res. Lett.*, **39**, L20702, doi:10.1029/2012GL053409.

Ashfaq, M., Y. Shi, W.-W. Tung, R. J. Trapp, X. Gao, J. S. Pal, and N. S. Diffenbaugh, 2009: Suppression of south Asian summer monsoon precipitation in the 21st century. *Geophys. Res. Lett.*, **36**, L01704, doi:10.1029/2008GL036500.

BAAQMD, 2014: Challenging "Winter Spare the Air" season comes to a close. Bay Area Air Quality Management District, press release, 4 March 2014. [Available online at http://www.baaqmd.gov/~/media/Files/Communications%20and%20Outreach/Publications/News%20Releases/2014/2014-019-WSTA-SEASON-ENDS-030414.ashx?la=en.]

Bacmeister, J. T., M. J. Suarez, and F. R. Robertson, 2006: Rain reevaporation, boundary layer–convection interactions, and Pacific rainfall patterns in an AGCM. *J. Atmos. Sci.*, **63**, 3383–3403.

——, M. F. Wehner, R. B. Neale, A. Gettelman, C. Hannay, P. H. Lauritzen, J. M. Caron, and J. E. Truesdale, 2014: Exploratory high-resolution climate simulations using the Community Atmosphere Model (CAM). *J. Climate*, **27**, 3073–3099.

Balmaseda, M. A., L. Ferranti, F. Molteni, and T. N. Palmer, 2010: Impact of 2007 and 2008 Arctic ice anomalies on the atmospheric circulation: Implications for long-range predictions. *Quart. J. Roy. Meteor. Soc.*, **136**, 1655–1664.

Barnett, T. P., and Coauthors, 2008: Human-induced changes in the hydrology of the western United States. *Science*, **319**, 1080–1083.

Barriopedro, D., E. M. Fischer, J. Lutenbacher, R. M. Trigo, and R. Garcia-Herrera, 2011: The hot summer of 2010: redrawing the temperature record map of Europe. *Science*, **332**, 220–224.

Becker, A., P. Finger, A. Meyer-Christoffer, B. Rudolf, K. Schamm, U. Schneider, and M. Ziese, 2013: A description of the global land-surface precipitation data products of the Global Precipitation Climatology Centre with sample applications including centennial (trend) analysis from 1901 to present. *Earth Syst. Sci. Data*, **5**, 71–99.

Berg, P., J. O. Haerter, P. Thejll, C. Piani, S. Hagemann, and J. H. Christensen, 2009: Seasonal characteristics of the relationship between daily precipitation intensity and surface temperature. *J. Geophys. Res.*, **114**, D18102, doi:10.1029/2009JD012008.

BfG-DWD, 2013: Länderübergreifende Analyse des Juni-Hochwassers 2013. Bundesanstalt für Gewässerkunde, 69 pp. [Available online at http://www.vhw.de/fileadmin/user_upload/Themenfelder/Umweltrecht/2013_09_04_pm_bfg-bericht.pdf.]

Bhend, J., and P. Whetton, 2013: Consistency of simulated and observed regional changes in temperature, sea level pressure and precipitation. *Climatic Change*, **118**, 799–810, doi:10.1007/s10584-012-0691-2.

Bindoff, N. L., and Coauthors, 2014: Detection and attribution of climate change: From global to regional. *Climate Change 2013: The Physical Science Basis*, T. F. Stocker et al., Eds., Cambridge University Press, 867–952.

Blackham, M., 2013: Dust bowled. *Water Atmos.*, **8**, 12–21.

Bladé, I., B. Liebmann, D. Fortuny, and G. J. Oldenborgh, 2012: Observed and simulated impacts of the summer NAO in Europe: Implications for projected drying in the Mediterranean region. *Climate Dyn.*, **39**, 709–727, doi:10.1007/s00382-011-1195-x.

Blunden, J., and D. S. Arndt, Eds., 2014: State of the Climate in 2013. *Bull. Amer. Meteor. Soc.*, **95** (7), S1–S257.

Boé, J., L. Terray, C. Cassou, and J. Najac, 2009: Uncertainties in European summer precipitation changes: Role of large scale circulation. *Climate Dyn.*, **33**, 265–276, doi:10.1007/s00382-008-0474-7.

Borah, N., A. K. Sahai, R. Chattopadhyay, S. Joseph, S. Abhilash, and B. N. Goswami, 2013: A self-organizing map–based ensemble forecast system for extended range prediction of active/break cycles of Indian summer monsoon. *J. Geophys. Res. Atmos.*, **118**, 9022–9034, doi:10.1002/jgrd.50688.

Buisán, S. T., M. A. Sanz, and J. I. López-Moreno, 2014: Spatial and temporal variability of winter snow and precipitation days in the western and central Spanish Pyrenees. *Int. J. Climatol.*, in press, doi:10.1002/joc.3978.

Bureau of Meteorology, 2012: State of the Climate 2012. [Available online at http://www.csiro.au/Outcomes/Climate/Understanding/State-of-the-Climate-2012.aspx.]

——, 2013a: Extreme heat in January 2013. Bureau of Meteorology Special Climate Statement 43, 19 pp. [Available online at http://www.bom.gov.au/climate/current/statements/scs43e.pdf.]

——, 2013b: Australia's warmest September on record. Bureau of Meteorology Special Climate Statement 46, 26 pp. [Available online at http://www.bom.gov.au/climate/current/statements/scs46.pdf.]

——, 2014: Annual Climate Report 2013. Bureau of Meteorology (Australia), 31 pp. [Available online at http://www.bom.gov.au/climate/annual_sum/2013/index.shtml.]

CAL FIRE, 2014: Drought prompts CAL FIRE to increase statewide staffing: Expected prolonged, elevated threat of wildfire due to dry conditions. CAL FIRE, news release, 28 January 2014. [Available online at http://www.fire.ca.gov/communications/downloads/newsreleases/2014/2014_Drought_Staffing.pdf.]

Carrera, M., R. Higgins, and V. Kousky, 2004: Downstream weather impacts associated with atmospheric blocking over the northeast Pacific. *J. Climate*, **17**, 4823–4840.

Cassou, C., 2008: Intraseasonal interaction between the Madden–Julian Oscillation and the North Atlantic Oscillation. *Nature*, **455**, 523–527.

Cattiaux, J., and P. Yiou, 2012: Contribution of atmospheric circulation to remarkable European temperatures of 2011. *Bull. Amer. Meteor. Soc.*, **93**, 1054–1057.

——, R. Vautard, C. Cassou, P. Yiou, V. Masson-Delmotte, and F. Codron, 2010: Winter 2010 in Europe: A cold extreme in a warming climate. *Geophys. Res. Lett.*, **37**, L20704, doi:10.1029/2010gl044613.

Cayan, D., and J. Roads, 1984: Local relationships between United States West Coast precipitation and monthly mean circulation parameters. *Mon. Wea. Rev.*, **112**, 1276–1282.

CDFW, 2014: CDFW puts closures in effect on some rivers, recommends further changes to the Fish and Game Commission. *California Department of Fish and Wildlife News*, 29 January 2014. [Available online at http://cdfgnews.wordpress.com/2014/01/29/cdfw-puts-closures-in-effect-on-some-rivers-recommends-further-changes-to-the-fish-and-game-commission.]

Chattopadhyay, R., A. K. Sahai, and B. N. Goswami, 2008: Objective identification of nonlinear convectively coupled phases of monsoon intraseasonal oscillation: Implications for prediction. *J. Atmos. Sci.*, **65**, 1549–1569.

Chen, S., and D. Cayan, 1994: Low-frequency aspects of the large-scale circulation and West Coast United States temperature/precipitation fluctuations in a simplifed general circulation model. *J. Climate*, **7**, 1668–1683.

Christidis, N., and P. A. Stott, 2014: Change in the odds of warm years and seasons due to anthropogenic influence on the climate. *J. Climate*, **27**, 2607–2621.

——, ——, and S. J. Brown, 2011: The role of human activity in the recent warming of extremely warm daytime temperatures. *J. Climate*, **24**, 1922–1930.

——, ——, G. S. Jones, H. Shiogama, T. Nozawa, and J. Luterbacher, 2012: Human activity and warm seasons in Europe. *Int. J. Climatol.*, **32**, 225–239.

——, ——, A. A. Scaife, A. Arribas, G. S. Jones, D. Copsey, J. R. Knight, and W. J. Tennant, 2013: A new HadGEM3-A-based system for attribution of weather- and climate-related extreme events. *J. Climate*, **26**, 2756–2783.

CIB, cited 2013: Central European flooding 2013. EURO4M Climate Indicator Bulletin. [Available online at http://cib.knmi.nl/mediawiki/index.php/Central_European_flooding_2013.]

Clark, A., B. Mullan, and A. Porteous, 2011: Scenarios of regional drought under climate change. National Institute of Water & Atmospheric Research, 135 pp. [Available online at http://www.niwa.co.nz/sites/niwa.co.nz/files/slmacc_drought_sldr093_june2011.pdf.]

CMA, 2014: *China Climate Bulletin for 2013.* China Meteorological Administration, 50 pp.

Compo, G. P., and P. D. Sardeshmukh, 2010: Removing ENSO-related variations from the climate record. *J. Climate*, **23**, 1597–1978.

Coumou, D., and S. Rahmstorf, 2012: A decade of weather extremes. *Nature Climate Change*, **2**, 491–496, doi:10.1038/NCLIMATE1452.

Dai, A., 2008: Temperature and pressure dependence of the rain-snow phase transition over land and ocean. *Geophys. Res. Lett.*, **35**, L12802, doi:10.1029/2008GL033295.

——, 2011: Drought under global warming: a review. *Wiley Interdiscip. Rev.: Climate Change*, **2**, 45–65.

——, 2013: The influence of the Inter-decadal Pacific Oscillation on US precipitation during 1923-2010. *Climate Dyn.*, **41**, 633–646.

Daithi, S., 2013: Boundary conditions for the C20C Detection and Attribution project: The ALL-Hist/est1 and NAT-Hist/CMIP5-est1 scenarios. International CLIVAR C20C+ Detection and Attribution Project, 18 pp. [Available online at http://portal.nersc.gov/c20c/input_data/C20C-DandA_dSSTs_All-Hist-est1_Nat-Hist-CMIP5-est1.pdf.]

Dangendorf, S., S. Müller-Navarra, J. Jensen, F. Schenk, T. Wahl, and R. Weisse, 2014: North Sea storminess from a novel storm surge record since AD 1843. *J. Climate*, **27**, 3582–3595.

Dee, D. P., and Coauthors, 2011: The ERA-Interim reanalysis: Configuration and performance of the data assimilation system. *Quart. J. Roy. Meteor. Soc.*, **137**, 553–597, doi:10.1002/qj.828.

DEFRA, 2013: Defra to meet the cost of removing sheep killed in snow, Department for Environment, Food & Rural Affairs, press release, 15 May 2013. [Available online at https://www.gov.uk/government/news/defra-to-meet-the-cost-of-removing-sheep-killed-in-snow.]

Deser, C., A. S. Phillips, and M. A. Alexander, 2010: Twentieth century tropical sea surface temperature trends revisited. *Geophys. Res. Lett.*, **37**, L10701, doi:10.1029/2010GL043321.

Deutschländer, T., K. Friedrich, S. Haeseler, and C. Lefebvre, 2013: Severe storm XAVER across northern Europe from 5 to 7 December 2013. Deutscher Wetterdienst, 19 pp. [Available online at http://www.dwd.de/bvbw/generator/DWDWWW/Content/Oeffentlichkeit/KU/KU2/KU24/besondere__ereignisse__global/stuerme/englischeberichte/201312__XAVER__europe,templateId=raw,property=publicationFile.pdf/201312_XAVER_europe.pdf.]

Dobhal, D. P., A. K. Gupta, M. Mehta, and D. D. Khandelwal, 2013: Kedarnath disaster: Facts and plausible causes. *Current Sci.*, **105**, 171–174.

Dole, R., J. Perlwitz, J. Eischeid, P. Pegion, T. Zhang, X. W. Quan, T. Xu, and D. Murray, 2011: Was there a basis for anticipating the 2010 Russian heat wave? *Geophys. Res. Lett.*, **38**, L06702, doi:10.1029/2010GL046582.

Donat, M. G., and Coauthors, 2013: Updated analyses of temperature and precipitation extreme indices since the beginning of the twentieth century: The HadEX2 dataset. *J. Geophys. Res. Atmos.*, **118**, 2098–2118, doi:10.1002/jgrd.50150.

Dong, B.-W., R. T. Sutton, and T. Woollings, 2013a: The extreme European summer 2012 (in "Explaining Extreme Events of 2012 from a Climate Perspective"). *Bull. Amer. Meteor. Soc.*, **94** (9), S28–S32.

——, ——, ——, and K. Hodges, 2013b: Variability of the North Atlantic summer stormtrack: Mechanisms and impacts. *Environ. Res. Lett.*, **8**, 034037, doi:10.1088/1748-9326/8/3/034037.

Douville, H., S. Bielli, C. Cassou, M. Dequé, N. M. J. Hall, S. Tyteca, and A. Voldoire, 2011: Tropical influence on boreal summer mid-latitude stationary waves. *Climate Dyn.*, **38**, 1783–1798.

Dube, A., R. Ashrit, A. Ashish, K. Sharma, G. R. Iyengar, E. N. Rajagopal, and S. Basu, 2013: Performance of NCMRWF forecast models in predicting the Uttarakhand heavy rainfall event during 17–18 June 2013. [India] National Centre for Medium Range Weather Forecasting Research Report NMRF/RR/08/2013, 35 pp. [Available online at http://www.ncmrwf.gov.in/ncmrwf/KEDARNATH_REPORT_FINAL.pdf.]

——, ——, ——, ——, ——, ——, and ——, 2014: Forecasting the heavy rainfall during Himalayan flooding - June 2013. *Wea. Climate Extremes*, **4**, 22–34, doi:10.1016/j.wace.2014.03.004.

Dubey, C. S., D. P. Shukla, A. S. Ningreichon, and A. L. Usham, 2013: Orographic control of the Kedarnath disaster. *Current Sci.*, **105**, 1474–1476.

Durga Rao, K. H. V., V. Venkateshwar Rao, V. K. Dadhwal, and P. G. Diwakar, 2014: Kedarnath flash floods: A hydrological and hydraulic simulation study. *Current Sci.*, **106**, 598–603.

DWR, 2013: DWR experimental winter outlook for water year 2014: Sees mostly dry conditions for California. California Department of Water Resources, news release, 27 November 2013. [Available online at http://www.water.ca.gov/news/newsreleases/2013/112513.pdf.]

——, 2014: DWR drops state water project allocation to zero, seeks to preserve remaining supplies. California Department of Water Resources, news release, 31 January 2014. [Available online at http://www.water.ca.gov/news/newsreleases/2014/013114pressrelease.pdf.]

El Kenawy, A., J. I. López-Moreno, and S. M. Vicente-Serrano, 2012: Trend and variability of surface air temperature in northeastern Spain (1920-2006): Linkage to atmospheric circulation. *Atmos. Res.*, **106**, 159–180.

Favre, A., and A. Gershunov, 2009: North Pacific cyclonic and anticyclonic transients in a global warming context: Possible consequences for Western North American daily precipitation and temperature extremes. *Climate Dyn.*, **32**, 969–987.

Feser, F., R. Weisse, and H. von Storch, 2001: Multi-decadal atmospheric modeling for Europe yields multi-purpose data. *Eos, Trans. Amer. Geophys. Union*, **82**, 305–310.

——, M. Barcikowska, O. Krueger, F. Schenk, R. Weisse, and L. Xia, 2014: Storminess over the North Atlantic and northwestern Europe - A review. *Quart. J. Roy. Meteor. Soc.*, in press, doi:10.1002/qj.2364.

Field, C. B., and Coauthors, Eds., 2012: *Managing the Risks of Extreme Events and Disasters to Advance Climate Change Adaptation*. Cambridge University Press, 582 pp.

Fischer, E. M., U. Beyerle, and R. Knutti, 2013: Spatial aggregation reveals robust projections in climate extremes. *Nature Climate Change*, **3,** 1033–1038, doi:10.1038/NCLIMATE2051.

Folland, C. K., J. Knight, H. W. Linderholm, D. Fereday, S. Ineson, and J. W. Hurrell, 2009: The summer North Atlantic oscillation: Past, present, and future. *J. Climate*, **22**, 1082–1103.

Francis, J. A., and S. J. Vavrus, 2012: Evidence linking Arctic amplification to extreme weather in mid-latitudes. *Geophys. Res. Lett.*, **39**, L06801, doi:10.1029/2012GL051000.

Franke, R., 2009: Die nordatlantischen Orkantiefs seit 1956. *Naturwiss. Rundsch.*, **62**, 349–356, updated.

Fyfe, J. C., N. P. Gillett, and G. J. Marshall, 2012: Human influence on extratropical southern hemisphere summer precipitation. *Geophys. Res. Lett.*, **39**, L23711, doi:10.1029/2012GL054199.

——, ——, and F. W. Zwiers, 2013: Overestimated global warming over the past 20 years. *Nature Climate Change*, **3**, 767–769.

Gershunov, A., and D. Cayan, 2003: Heavy daily precipitation frequency over the contiguous United States: Sources of climatic variability and seasonal predictability. *J. Climate*, **16**, 2752–2765.

Geyer, B., 2014: High-resolution atmospheric reconstruction for Europe 1948–2012: coastDat2. *Earth Sys. Sci. Data*, **6**, 147–164, doi:10.5194/essd-6-147-2014.

Ghosh, S., D. Das, S.-C. Kao, and A. R. Ganguly, 2012: Lack of uniform trends but increasing spatial variability in observed Indian rainfall extremes. *Nature Climate Change*, **2**, 86–91.

Goswami, B. N., V. Venugopal, D. Sengupta, M. S. Madhusoodanan, and P. K. Xavier, 2006: Increasing trend of extreme rain events over India in a warming environment. *Science*, **314**, 1442–1445.

Graham, R. A., and R. H. Grumm, 2010: Utilizing normalized anomalies to assess synoptic-scale weather events in the western United States. *Wea. Forecasting*, **25**, 428–445.

Grams, C. M., H. Binder, S. Pfahl, N. Piaget, and H. Wernli, 2014: Atmospheric processes triggering the central European floods in June 2013. *Nat. Hazards Earth Syst. Sci.*, **14**, 1691–1702, doi:10.5194/nhess-14-1691-2014.

Graves, C. E., J. T. Moore, M. J. Singer, and S. Ng, 2003: Band on the run - Chasing the physical processes associated with heavy snowfall. *Bull. Amer. Meteor. Soc.*, **84**, 990–994.

Grumm, R. H., and R. Hart, 2001: Standardized anomalies applied to significant cold season weather events: Preliminary findings. *Wea. Forecasting*, **16**, 736–754.

Haeseler, S., and Coauthors, 2013: Heavy storm CHRISTIAN on 28 October 2013. Deutscher Wetterdienst, 20 pp. [Available online at http://www.dwd.de/bvbw/generator/DWDWWW/Content/Oeffentlichkeit/KU/KU2/KU24/besondere__ereignisse__global/stuerme/englischeberichte/20131028__CHRISTIAN__europe,templateId=raw,property=publicationFile.pdf/20131028_CHRISTIAN_europe.pdf.]

Hamill, T., 2014: Performance of operational model precipitation forecast guidance during the 2013 Colorado Front-Range floods. *Mon. Wea. Rev.*, **142**, 2609–2618.

Hansen, W. R., B. J. Chronic, and J. Matelock, 1978: Climatography of the Front Range urban corridor and vicinity, Colorado. USGS Professional Paper 1019, 59 pp. [Available online at http://pubs.usgs.gov/pp/1019/report.pdf.]

Hart, R. E., and R. H. Grumm, 2001: Using normalized climatological anomalies to rank synoptic-scale events objectively. *Mon. Wea. Rev.*, **129**, 2426–2442.

Hartmann, D. L., and Coauthors, 2014: Observations: Atmosphere and surface. *Climate Change 2013: The Physical Science Basis,* T. F. Stocker et al., Eds., Cambridge University Press, 159–254.

Hasselmann, K., 1979: On the signal-to-noise problem in atmospheric response studies. *Meteorology over the Tropical Oceans*, B. D. Shaw, Ed., Royal Meteorological Society, 251–259.

Haylock, M. R., N. Hofstra, A. M. G. Klein Tank, E. J. Klok, P. D. Jones, and M. New, 2008: A European daily high-resolution gridded dataset of surface temperature and precipitation for 1950–2006. *J. Geophys. Res.*, **113**, D20119, doi:10.1029/2008JD010201.

Hegerl, G., and F. Zwiers, 2011: Use of models in detection and attribution of climate change. *Wiley Interdiscip. Rev.: Climate Change*, **2**, 570–591.

——, O. Hoegh-Guldberg, G. Casassa, M. P. Hoerling, R. S. Kovats, C. Parmesan, D. W. Pierce, and P. A. Stott, 2009: Good practice guidance paper on detection and attribution related to anthropogenic climate change. IPCC Expert Meeting on Detection and Attribution Related to Anthropogenic Climate Change, T. F. Stocker et al., Eds., University of Bern, Switzerland, 1–8. [Available online at https://www.ipcc-wg1.unibe.ch/guidancepaper/IPCC_D&A_GoodPracticeGuidancePaper.pdf.]

Hendon, H. H., D. W. J. Thompson, and M. C. Wheeler, 2007: Australian rainfall and surface temperature variations associated with the Southern Hemisphere annular mode. *J. Climate*, **20**, 2452–2467.

——, E.-P. Lim, J. M. Arblaster, and D. T. L. Anderson 2014: Causes and predictability of the record wet spring over Australia in 2010. *Climate Dyn.,* **42**, 1155–1174.

Hewitson, B. C., and R. G. Crane, 2002: Self-organizing maps: Applications to synoptic climatology. *Climate Res.*, **22**, 13–26.

Hewitt, H. T., D. Copsey, I. D. Culverwell, C. M. Harris, R. S. R. Hill, A. B. Keen, A. J. McLaren, and E. C. Hunke, 2011: Design and implementation of the infrastructure of HadGEM3: The next-generation Met Office climate modelling system. *Geosci. Model Dev.*, **4**, 223–253.

Hirabayashi, Y., R. Mahendran, S. Koirala, L. Konoshima, D. Yamazaki, S. Watanabe, H. Kim, and S. Kanaes, 2013: Global flood risk under climate change. *Nature Climate Change*, **3**, 816–821.

Hirsch, R. M., and K. R. Ryberg, 2012: Has the magnitude of floods across the USA changed with global CO2 levels? *Hydrolog. Sci. J.*, **57**, 1–9, doi:10.1080/02626667.2011.621895.

Hoerling, M., J. Eischeid, J. Perlwitz, X. Quan, T. Zhang, and P. Pegion, 2012: On the increased frequency of Mediterranean drought. *J. Climate*, **25**, 2146–2161.

——, and Coauthors, 2013: Anatomy of an extreme event. *J. Climate*, **26**, 2811–2832.

Hong, C.-C., H.-H. Hsu, N.-H. Lin, and H. Chiu, 2011: Roles of European blocking and tropical-extratropical interaction in the 2010 Pakistan flooding. *Geophys. Res. Lett.*, **38**, L13806, doi:10.1029/2011GL047583.

Hoskins, B. J., and K. I. Hodges, 2002: New perspectives on the Northern Hemisphere winter storm tracks. *J. Atmos. Sci.*, **59**, 1041–1061.

Houze, R. A., K. L. Rasmussen, S. Medina, S. R. Brodzik, and U. Romatschke, 2011: Anomalous atmospheric events Leading to the summer 2010 floods in Pakistan. *Bull. Amer. Meteor. Soc.*, **92**, 291–298.

HPRC, cited 2014: High Plains Regional Center - Current climate summary maps. [Available online at http://www.hprcc.unl.edu/.]

Hudson, D., A. G. Marshall, Y. Yin, O. Alves, and H. H. Hendon, 2013: Improving intraseasonal prediction with a new ensemble generation strategy. *Mon. Wea. Rev.*, **141**, 4429–4449.

Huffington Post, 2014: The costs of California's bellwether drought: What can we expect? [Available online at http://www.huffingtonpost.com/peter-h-gleick/the-costs-of-californias_b_4747043.html.]

Hurrell, J. W., and C. Deser, 2009: North Atlantic climate variability: The role of the North Atlantic Oscillation. *J. Marine Sys.*, **79**, 231–244.

——, and Coauthors, 2013: The Community Earth System Model: A framework for collaborative research. *Bull. Amer. Meteor. Soc.*, **94**, 1339–1360.

Johnson, N. C., 2013: How many ENSO flavors can we distinguish? *J. Climate*, **26**, 4816–4827.

Jones, D. A., W. Wang, and R. Fawcett, 2009: High-quality spatial climate data-sets for Australia. *Aust. Meteor. Oceanogr. J.*, **58**, 233–248.

Jones, P. D., D. H. Lister, T. J. Osborn, C. Harpham, M. Salmon, and C. P. Morice, 2012: Hemispheric and large-scale land surface air temperature variations: An extensive revision and an update to 2010. *J. Geophys. Res.*, **117**, D05127, doi:10.1029/2011JD017139.

Joseph, S., and Coauthors, 2014: North Indian heavy rainfall event during June 2013: Diagnostics and extended range prediction. *Climate Dyn.*, in press, doi:10.1007/s00382-014-2291-5.

Junker, N. W., R. H. Grumm, R. Hart, L. F. Bosart, K. M. Bell, and F. J. Pereira, 2008: Use of normalized anomaly fields to anticipate extreme rainfall in the mountains of northern California. *Wea. Forecasting*, **23**, 336–356.

Jurewicz, M. L., and M. S. Evans, 2004: A comparison of two banded, heavy snowstorms with very different synoptic settings. *Wea. Forecasting*, **19**, 1011–1028.

Kalnay, E., and Coauthors, 1996: The NCEP/NCAR 40-Year Reanalysis Project. *Bull. Amer. Meteor. Soc.*, **77**, 437–471.

Karoly, D. J., 2009: The recent bushfires and extreme heat wave in southeast Australia. *Bull. Aust. Meteor. Oceanogr. Soc.*, **22**, 10–13.

——, and K. Braganza, 2005: A new approach to detection of anthropogenic temperature changes in the Australian region. *Meteor. Atmos. Phys.,* **89**, 57–67.

——, and Coauthors, 2012: Science underpinning the prediction and attribution of extreme events. WCRP Grand Challenge white paper, 5 pp. [Available online at http://www.wcrp-climate.org/documents/GC_Extremes.pdf.]

Kerr, R., 2013: In the hot seat. *Science*, **342**, 688–689.

Kim, Y. H., M.-K. Kim, and W.-S. Lee, 2008: An investigation of large-scale climate indices with the influence of temperature and precipitation variation in Korea. *Atmosphere*, **18**, 83–95. (In Korean with English abstract.)

Kistler, R., and Coauthors, 2001: The NCEP-NCAR 50-year reanalysis: Monthly means CD-ROM and documentation. *Bull. Amer. Meteor. Soc.*, **82**, 247–267.

Klein-Tank, A. M. G., and Coauthors, 2002: Daily dataset of 20th-century surface air temperature and precipitation series for the European Climate Assessment. *Int. J. Climatol.*, **22**, 1441–1453.

Knutson, T. R., F. Zeng, and A. T. Wittenberg, 2013a: Multimodel assessment of regional surface temperature trends: CMIP3 and CMIP5 Twentieth Century simulations. *J. Climate*, **26**, 8709–8743.

——, ——, and ——, 2013b: The extreme March 2012 warm anomaly over the eastern United States: Global context and multimodel trend analysis [in "Explaining Extreme Events of 2012 from a Climate Perspective"]. *Bull. Amer. Meteor. Soc.*, **94** (9), S13–S17.

Knutti, R., and J. Sedláček, 2013: Robustness and uncertainties in the new CMIP5 climate model projections. *Nature Climate Change*, **3**, 369–373.

Kohonen, T., 2001: *Self-Organizing Maps.* 3rd ed. Springer Series in Information Sciences, Vol. 30, Springer, 501 pp.

Krishnamurthy, C. K. B., U. Lall, and H.-H. Kwon, 2009: Changing frequency and intensity of rainfall extremes over India from 1951 to 2003. *J. Climate*, **22**, 4737–4746.

Kumar, A., H. Wang, W. Wang, Y. Xue, and Z.-Z. Hu, 2013: Does knowing the oceanic PDO phase help predict the atmospheric anomalies in subsequent months? *J. Climate*, **26**, 1268–1285.

Kunkel, K. E., and Coauthors, 2013: Monitoring and understanding trends in extreme storms: State of knowledge. *Bull. Amer. Meteor. Soc.*, **94**, 499–514.

Lamarque, J.-F., and Coauthors, 2010: Historical (1850–2000) gridded anthropogenic and biomass burning emissions of reactive gases and aerosols: Methodology and application. *Atmos. Chem. Phys.*, **10**, 7017–7039, doi:10.5194/acp-10-7017-2010.

Langford, S., S. Stevenson, and D. Noone, 2014: Analysis of low-frequency precipitation variability in CMIP5 historical simulations for southwestern North America. *J. Climate*, **27**, 2735–2756.

Lau, W. K. M., and K.-M. Kim, 2011: The 2010 Pakistan flood and Russian heat wave: Teleconnection of hydrometeorological extremes. *J. Hydrometeor.*, **13**, 392–403.

Lewis, S. C., and D. J. Karoly, 2013: Anthropogenic contributions to Australia's record summer temperatures of 2013. *Geophys. Res. Lett.*, **40**, 3705–3709, doi:10.1002/grl.50673.

Li, C., and M. Yanai, 1996: The onset and interannual variability of the Asian summer monsoon in relation to land–sea thermal contrast. *J. Climate*, **9**, 358–375.

Li, H., J. Sheffield, and E. F. Wood, 2010a: Bias correction of monthly precipitation and temperature fields from Intergovernmental Panel on Climate Change AR4 models using equidistant quantile matching. *J. Geophys. Res.*, **115**, D10101, doi:10.1029/2009JD012882.

——, A. Dai, T. Zhou, and J. Lu, 2010b: Responses of East Asian summer monsoon to historical SST and atmospheric forcing during 1950–2000. *Climate Dyn.*, **34**, 501–514.

Lindenberg, J., H.-T. Mengelkamp, and G. Rosenhagen, 2012: Representativity of near surface wind measurements from coastal stations at the German Bight. *Meteor. Z.*, **21**, 99–106.

López-Moreno, J. I., 2005: Recent variations of snowpack depth in the Central Spanish Pyrenees. *Arct. Antarct. Alp. Res.*, **37**, 253–260.

——, and S. M. Serrano-Vicente, 2007: Atmospheric circulation influence on the interannual variability of snowpack in the Spanish Pyrenees during the second half of the twentieth century. *Nordic Hydrol.*, **38**, 38–44.

——, ——, and S. Lanjeri, 2007: Mapping of snowpack distribution over large areas using GIS and interpolation techniques. *Climate Res.*, **33**, 257–270.

——, ——, S. Beguería, A. M. El Kenawy, and M. Angulo, 2010: Trends in daily precipitation on the north-eastern Iberian Peninsula, 1955-2006. *Int. J. Climatol.*, **120**, 248–257.

Lorenz, R., E. B. Jaeger, and S. I. Seneviratne, 2010: Persistence of heat waves and its link to soil moisture memory. *Geophys. Res. Lett.*, **37**, L09703, doi:10.1029/2010GL042764.

Lott, F. C., N. Christidis, and P. A. Stott, 2013: Can the 2011 East African drought be attributed to human-induced climate change? *Geophys. Res. Lett.*, **40**, 1177–1181.

Mantua, N. J., S. R. Hare, Y. Zhang, J. M. Wallace, and R. C. Francis, 1997: A Pacific interdecadal climate oscillation with impacts on salmon production. *Bull. Amer. Meteor. Soc.*, **78**, 1069–1079.

Marshall, A. G., D. Hudson, M. C. Wheeler, O. Alves, H. H. Hendon, M. J. Pook, and J. S. Risbey, 2013: Intra-seasonal drivers of extreme heat over Australia in observations and POAMA-2. *Climate Dyn.*, doi:10.1007/s00382-013-2016-1.

Martin, J. E., 1999: Quasigeostrophic forcing of ascent in the occluded sector of cyclones and the trowal airstream. *Mon. Wea. Rev.*, **127**, 70–88.

Marty, C., 2008: Regime shift of snow days in Switzerland. *Geophys. Res. Lett.*, **35**, L12501, doi:10.1029/2008GL033998.

Marvel, K., and C. Bonfils, 2013: Identifying external influences on global precipitation. *Proc. Natl. Acad. Sci. USA*, **110**, 19301–19306.

Massey, N., and Coauthors, 2014: weather@home – development and validation of a very large ensemble modelling system for probabilistic event attribution. *Quart. J. Roy. Meteor. Soc.*, in press, doi:10.1002/qj.2455.

Mastrandrea, M. D., K. J. Mach, G.-K. Plattner, O. Edenhofer, T. F. Stocker, C. B. Field, K. L. Ebi, and P. R. Matschoss, 2011: The IPCC AR5 guidance note on consistent treatment of uncertainties: a common approach across the working groups. *Climate Change*, **108**, 675–691.

Matulla, C., W. Schöner, H. Alexandersson, H. von Storch, and X. Wang, 2007: European storminess: Late nineteenth century to present. *Climate Dyn.*, **31**, 125–130.

Mayes, B. E., J. M. Boustead, M. O'Malley, S. M. Fortin, and R. H. Grumm, 2009: Utilizing standardized anomalies to assess synoptic scale weather events in the central United States. Preprints, *23rd Conf. on Weather Analysis and Forecasting*, Omaha, NE, Amer. Meteor. Soc., 16B.3. [Available online at http://ams.confex.com/ams/pdfpapers/154217.pdf.]

McCabe, G. J., and M. D. Dettinger, 1999: Decadal variations in the strength of ENSO teleconnections with precipitation in the western United States. *Int. J. Climatol.*, **19**, 1399–1410.

McKee, T. B., and N. J. Doesken, 1997: Colorado Extreme Storm Precipitation Data Study. Climatology Rep. 97-1, Colorado Climate Center, Colorado State University, 109 pp. [Available online at http://climate.colostate.edu/pdfs/Climo_97-1_Extreme_ppt.pdf.]

Menne, M., I. Durre, R. Vose, B. Gleason, and T. Houston, 2012: An overview of the Global Historical Climatology Network-Daily database. *J. Atmos. Oceanic Technol.*, **29**, 897–910.

Met Office, cited 2014: Hot dry spell July 2013. [Available online at http://www.metoffice.gov.uk/climate/uk/interesting/2013-heatwave.]

Michelangeli, P.-A., R. Vautard, and B. Legras, 1995: Weather regimes: Recurrence and quasi-stationarity. *J. Atmos. Sci.*, **52**, 1237–1256.

Min, S.-K., X. Zhang, F. W. Zwiers, and G. C. Hegerl, 2011: Human contribution to more-intense precipitation extremes. *Nature*, **470**, 378–381, doi:10.1038/nature09763.

——, ——, ——, H. Shiogama, Y.-S. Tung, and M. Wehner, 2013: Multi-model detection and attribution of extreme temperature changes. *J. Climate*, **26**, 7430–7451.

Mishra, A., and J. Srinivasan, 2013: Did a cloud burst occur in Kedarnath during 16 and 17 June 2013. *Current Sci.*, **105**, 1351–1352.

Mitchell, T., and W. Blier, 1997: The variability of wintertime precipitation in the region of California. *J. Climate*, **10,** 2261–2276.

Molod, A., L. Takacs, M. Suarez, J. Bacmeister, I.-S. Song, and A. Eichmann, 2012: The GEOS-5 Atmospheric General Circulation Model: Mean climate and development from MERRA to Fortuna**.** NASA Tech. Rep. Series on Global Modeling and Data Assimilation, NASA TM—2012-104606, Vol. 28, 117 pp.

Moore, J. T., C. E. Graves, S. Ng, and J. L. Smith, 2005: A process-oriented methodology toward understanding the organization of an extensive mesoscale snowband: A diagnostic case study of 4–5 December 1999. *Wea. Forecasting*, **20**, 35–50.

Morak, S., G. C. Hegerl, and J. Kenyon, 2011: Detectable regional changes in the number of warm nights. *Geophys. Res. Lett.*, **38**, L17703, doi:10.1029/2011GL048531.

——, ——, and N. Christidis, 2013: Detectable changes in the frequency of temperature extremes. *J. Climate*, **26**, 1561–1574.

Morice, C. P., J. J. Kennedy, N. A. Rayner, and P. D. Jones, 2012: Quantifying uncertainties in global and regional temperature change using an ensemble of observational estimates: The HadCRUT4 dataset. *J. Geophys. Res.*, **117**, D08101, doi:10.1029/2011JD017187.

Mudelsee, M., M. Börngen, G. Tetzlaff, and U. Grünewald, 2003: No upward trends in the occurrence of extreme floods in central Europe. *Nature*, **425**, 166–169.

Nairn, J., and R. Fawcett, 2013: Defining heatwaves: Heatwave defined as a heat impact event servicing all community and business sectors in Australia. CAWCR Technical Report No. 060, 84 pp. [Available online at http://www.cawcr.gov.au/publications/technicalreports/CTR_060.pdf.]

Namias, J., 1978a: Recent drought in California and western Europe. *Rev. Geophys.*, **16**, 435–458.

——, 1978b: Multiple causes of the North American abnormal winter 1976–1977. *Mon. Wea. Rev.*, **106**, 279–295.

NASA Earth Observatory, cited 2014: MODIS TERRA imagery. [Available online at http://earthobservatory.nasa.gov/IOTD/view.php?id=82910.]

NCDC, 2005: *Storm Data*. NOAA/NESDIS National Climatic Data Center, **47** (10), 132 pp. [Available online at http://www.ncdc.noaa.gov/IPS/sd/sd.html.]

NCLIMDIV, 2014: NOAA's gridded climate divisional dataset. National Climatic Data Center, Asheville, NC, digital media, retrieved 05 June 2014. [Available online at http://www.ncdc.noaa.gov/cag.]

Neelin, J. D., B. Langenbrunner, J. E. Meyerson, A. Hall, and N. Berg, 2013: California winter precipitation change under global warming in the Coupled Model Intercomparison Project Phase 5 ensemble. *J. Climate*, **26**, 6238–6256.

New Zealand Treasury, 2013: Budget economic and fiscal update 2013. New Zealand Treasury, 176 pp. [Available online at http://www.treasury.govt.nz/budget/forecasts/befu2013/befu13-whole.pdf.]

Nicholls, N., 2004: The changing nature of Australian droughts. *Climatic Change*, **63**, 323–336.

NIDIS, cited 2014: National Integrated Drought Information System drought portal. [Available online at http://www.drought.gov/drought/news/ca-governor-signs-687-million-drought-plan.]

Nitschke, M., G. R. Tucker, and P. Bi, 2007: Morbidity and mortality during heatwaves in metropolitan Adelaide. *Med. J. Aust.*, **187**, 662–665.

NOAA, 2013: State of the climate: Global analysis for May 2013. [Available online at http://www.ncdc.noaa.gov/sotc/global/2013/5.]

NOAA NCDC, 2014: National overview: February 2014. [Available online at https://www.ncdc.noaa.gov/sotc/national/2014/2.]

Novak, D. R., L. F. Bosart, D. Keyser, and J. S. Waldstreicher, 2004: An observational study of cold season–banded precipitation in northeast U.S. cyclones. *Wea. Forecasting*, **19**, 993–1010.

Ogawa, F., H. Nakamura, K. Nishii, T. Miyasaka, and A. Kuwano-Yoshida, 2012: Dependence of the climatological axial latitudes of the tropospheric westerlies and storm tracks on the latitude of an extratropical oceanic front. *Geophys. Res. Lett.*, **39**, L05804, doi:10.1029/2011GL049922.

O'Gorman, P. A., and T. Schneider, 2009: The physical basis for increases in precipitation extremes in simulations of 21st-century climate change. *Proc. Natl. Acad. Sci. USA*, **106**, 14773–14777.

Omrani, N.-E., N. S. Keenlyside, J. Bader, and E. Manzini, 2014: Stratosphere key for wintertime atmospheric response to warm Atlantic decadal conditions. *Climate Dyn.*, **42**, 649–663.

Onogi, K., and Coauthors, 2007: The JRA-25 reanalysis. *J. Meteor. Soc. Japan*, **85**, 369–432.

Otto, F. E. L., N. Massey, G. J. van Oldenborgh, R. G. Jones, and M. R. Allen, 2012: Reconciling two approaches to attribution of the 2010 Russian heat wave. *Geophys. Res. Lett.*, **39**, L04702, doi:10.1029/2011GL050422.

Pall, P., T. Aina, D. A. Stone, P. A. Stott, T. Nozawa, A. G. J. Hilberts, D. Lohmann, and M. R. Allen, 2011: Anthropogenic greenhouse gas contribution to flood risk in England and Wales in autumn 2000. *Nature*, **470**, 382–385, doi:10.1038/nature09762.

Pekárová, P., D. Halmová, V. B. Mitková, P. Miklánek, J. Pekár, and P. Škoda, 2013: Historic flood marks and flood frequency analysis of the Danube River at Bratislava, Slovakia. *J. Hydrol. Hydromech.*, **61**, 326–333.

Perkins, S. E., and L. V. Alexander, 2013: On the measurement of heat waves. *J. Climate*, **26**, 4500–4517.

——, and E. M. Fischer, 2013: The usefulness of different realizations from the model evaluation of regional trends in heat waves. *Geophys. Res. Lett.,* **40**, 5793–5797, doi:10.1002/2013GL057833.

Peters, G. P., and Coauthors, 2012: The challenge to keep global warming below 2°C. *Nature Climate Change*, **3**, 4–6, doi:10.1038/nclimate1783.

Peterson, T. C., and Coauthors, 2008: Why weather and climate extremes matter. *Weather and Climate Extremes in a Changing Climate. Regions of Focus: North America, Hawaii, Caribbean, and U.S. Pacific Islands.* T. R. Karl et al., Eds., U.S. Climate Change Science Program and the Subcommittee on Global Change Research, 11–33.

Petoukhov, V., and V. Semenov, 2010: A link between reduced Barents-Kara sea ice and cold winter extremes over northern continents. *J. Geophys. Res.*, **115**, D21111, doi:10.1029/2009JD013568.

——, S. Rahmstorf, S. Petri, and H. J. Schellnhuber, 2013: Quasiresonant amplification of planetary waves and recent Northern Hemisphere weather extremes. *Proc. Natl. Acad. Sci. USA*, **110**, 5336–5341.

Pierce, D. W., 2002: The role of sea surface temperatures in interactions between ENSO and the North Pacific oscillation. *J. Climate*, **15**, 1295–1308.

Pinto, J. G., N. Bellenbaum, M. K. Karremann, and P. M. Della-Marta, 2013: Serial clustering of extratropical cyclones over the North Atlantic and Europe under recent and future climate conditions. *J. Geophys. Res. Atmos.*, **118**, 12476–12485, doi:10.1002/2013JD020564.

Polade, S. D., A. Gershunov, D. R. Cayan, M. D. Dettinger, and D. W. Pierce, 2013: Natural climate variability and teleconnections to precipitation over the Pacific-North American region in CMIP3 and CMIP5 models. *Geophys. Res. Lett.*, **40**, 2296–2301.

——, D. W. Pierce, D. R. Cayan, A. Gershunov, and M. D. Dettinger, 2014: The key role of dry days in changing regional climate and precipitation regimes. *Sci. Rep.*, **4**, 4364, doi:10.1038/srep04364.

Pope, V. D., M. L. Gallani, P. R. Rowntree, and R. A. Stratton, 2000: The impact of new physical parametrizations in the Hadley Centre climate model: HadAM3. *Climate Dyn.*, **16**, 123–146, doi:10.1007/s003820050009.

Porteous, A., and B. Mullan, 2013: The 2012-13 drought: An assessment and historical perspective. MPI Tech. Paper No. 2012/18. Ministry for Primary Industries/National Institute of Water & Atmospheric Research, 57 pp. [Available online at http://www.niwa.co.nz/sites/niwa.co.nz/files/2013-18-The%202012-13%20drought%20an%20assessment%20and%20historical%20perspective.pdf.]

Power, S., T. Casey, C. Folland, A. Colman, and V. Mehta, 1999: Inter-decadal modulation of the impact of ENSO on Australia. *Climate Dyn.*, **15**, 319–324.

——, M. Haylock, R. Colman, and X. Wang, 2006: The predictability of interdecadal changes in ENSO activity and ENSO teleconnections. *J. Climate*, **19**, 4755–4771.

Prakash, S., 2013: Brief Report on visit to Alaknanda Valley, Uttarakhand Himalaya during 22-24 June 2013. [India] National Institute of Disaster Management, [12 pp.] [Available online at http://www.nidm.gov.in/pdf/Uttarakhand%20Disaster.pdf.]

PRISM, 2014: PRISM climate data. PRISM Climate Group, Oregon State University, Corvallis, OR, digital media, retrieved 10 Feb 2014. [Available online at http://prism.oregonstate.edu.]

Qian, C., and T. Zhou, 2014: Multidecadal variability of North China aridity and its relationship to PDO during 1900-2010. *J. Climate*, **27**, 1210–1222.

Qian, Y., L. Leung, S. Ghan, and F. Giorgi, 2003: Regional climate effects of aerosols over China: Modeling and observation. *Tellus*, **55B**, 914–934.

——, D. Gong, J. Fan, L. Leung, R. Bennartz, D. Chen, and W. Wang, 2009: Heavy pollution suppresses light rain in China: Observations and modeling. *J. Geophys. Res.*, **114**, D00K02, doi:10.1029/2008JD011575.

Rajeevan, M., S. Gadgil, and J. Bhate, 2010: Active and break spells of the Indian summer monsoon. *J. Earth Sys. Sci.*, **119**, 229–247.

Rayner, N. A., D. E. Parker, E. B. Horton, C. K. Folland, L. V. Alexander, D. P. Rowell, E. C. Kent, and A. Kaplan, 2003: Global analyses of sea surface temperature, sea ice, and night marine air temperature since the late nineteenth century. J. *Geophys. Res.*, **108** (D14), 4407, doi:10.1029/2002JD002670.

Rienecker, M. M., and Coauthors, 2008: The GEOS-5 data assimilation system—Documentation of versions 5.0.1, 5.1.0, and 5.2.0. NASA Tech. Rep. Series on Global Modeling and Data Assimilation, NASA/TM-2007-104606, Vol. 27, 95 pp.

——, and Coauthors, 2011: MERRA: NASA's Modern-Era Retrospective Analysis for Research and Applications. *J. Climate*, **24**, 3624–3648.

Rupp, D. E., P. W. Mote, N. Massey, C. J. Rye, R. Jones, and M. R. Allen, 2012: Did human influence on climate make the 2011 Texas drought more probable? [in "Explaining Extreme Events of 2011 from a Climate Perspective"]. *Bull. Amer. Meteor. Soc.*, **93**, 1052–1067.

——, ——, ——, F. E. L. Otto, and M. R. Allen, 2013: Human influence on the probability of low precipitation in the Central United States in 2012 [in "Explaining Extreme Events of 2012 from a Climate Perspective"]. *Bull. Amer. Meteor. Soc.*, **94** (9), S2–S6.

Sampe, T., H. Nakamura, A. Goto, and W. Ohfuchi, 2010: Significance of a midlatitude SST frontal zone in the formation of a storm track and an eddy-driven westerly jet. *J. Climate*, **23**, 1793–1814.

Schaer, C., P. L. Vidale, D. Luethi, C. Frei, C. Haeberli, M. A. Liniger, and C. Appenzeller, 2004: The role of increasing temperature variability in European summer heatwaves. *Nature*, **427**, 332–336.

Schmidt, H., and H. von Storch, 1993: German Bight storms analysed. *Nature*, **365**, 791–791.

Schneider, U., A. Becker, P. Finger, A. Meyer-Christoffer, M. Ziese, and B. Rudolf, 2014: GPCC's new land surface precipitation climatology based on quality-controlled in situ data and its role in quantifying the global water cycle. *Theor. Appl. Climatol.*, **115**, 15–40, doi:10.1007/s00704-013-0860-x.

Schubert, S., and Coauthors, 2009: A U.S. CLIVAR project to assess and compare the responses of global climate models to drought-related SST forcing patterns: Overview and results. *J. Climate*, **22**, 5251–5272.

——, H. Wang, R. Koster, M. Suarez, and P. Groisman, 2014: Northern Eurasian heat waves and droughts. *J. Climate,* **27**, 3169–3207.

Schwartz, R. M., and T. W. Schmidlin, 2002: Climatology of blizzards in the conterminous United States, 1959-2000. *J. Climate*, **15**, 1765–1772.

Screen, J. A., I. Simmonds, C. Deser, and R. Tomas, 2013: The atmospheric response to three decades of observed Arctic sea ice loss. *J. Climate*, **26**, 1230–1248.

Seneviratne, S. I., 2012: Climate science: Historical drought trends revisited. *Nature*, **491**, 338–339.

——, T. Corti, E. L. Davin, M. Hirschi, E. B. Jaeger, I. Lehner, B. Orlowsky, and A. J. Teuling, 2010: Investigating soil moisture-climate interactions in a changing climate: A review. *Earth-Sci. Rev.*, **99**, 125–161.

——, M. G. Donat, B. Mueller, and L. V. Alexander, 2014: No pause in the increase of hot temperature extremes. *Nature Climate Change*, **4**, 161–163, doi:10.1038/nclimate2145.

Sewall, J. O., 2005: Precipitation shifts over western North America as a result of declining Arctic sea ice cover: The coupled system response. *Earth Interact.*, **9**, 1–23, doi:10.1175/EI171.1.

Sheffield, J., E. F. Wood, and M. L. Roderick, 2012: Little change in global drought over the past 60 years. *Nature*, **491**, 435–438.

——, and Coauthors, 2013: North American climate in CMIP5 experiments. Part I: Evaluation of historical simulations of continental and regional climatology. *J. Climate*, **26**, 9209–9245.

Sherwood, S., and Q. Fu, 2014: A drier future? *Science*, **343**, 737–738.

Shiogama, H., M. Watanabe, Y. Imada, M. Mori, M. Ishii, and M. Kimoto, 2013: An event attribution of the 2010 drought in the south Amazon region using the MIROC5 model. *Atmos. Sci. Lett.*, **14**, 170–175.

Siderius, C., and Coauthors, 2013: Snowmelt contributions to discharge of the Ganges. *Sci. Total Environ.*, **468–469** (Suppl.), S93–S101, doi:10.1016/j.scitotenv.2013.05.084.

Sillmann, J., V. V. Kaharin, F. W. Zwiers, X. Zhang, and D. Bronaugh, 2013: Climate extreme indicies in the CMIP5 multimodel ensemble: Part 2. Future climate projections. *J. Geophys. Res. Atmos.*, **118**, 2473–2493, doi:10.1002/jgrd.50188.

——, M. G. Donat, J. C. Fyfe, and F. W. Zwiers, 2014: Observed and simulated temperature extremes during the recent warming hiatus. *Environ. Res. Lett.*, **9**, 064023, doi:10.1088/1748-9326/9/6/064023.

Singh, D., M. Tsiang, B. Rajaratnam, and N. S. Diffenbaugh, 2014: Observed changes in extreme wet and dry spells during the South Asian summer monsoon season. *Nature Climate Change*, **4**, 456–461.

Slingo, J., 2013: Why was the start to spring 2013 so cold? Met Office briefing note, April 2013. [Available online at http://www.metoffice.gov.uk/research/news/cold-spring-2013.]

Smith, T. M., R. W. Reynolds, T. C. Peterson, and J. Lawrimore, 2008: Improvements to NOAA's historical merged land-ocean surface temperature analysis (1880-2006). *J. Climate*, **21**, 2283–2296.

Solomon, A., and M. Newman, 2012: Reconciling disparate twentieth-century Indo-Pacific Ocean temperature trends in the instrumental record. *Nature Climate Change*, **2**, 691–699.

Song, F., T. Zhou, and Y. Qian, 2014: Responses of East Asian summer monsoon to natural and anthropogenic forcings in the 17 latest CMIP5 models. *Geophys. Res. Lett.*, **41**, 596–603, doi:10.1002/2013GL058705.

Sperber, K. R., H. Annamalai, I.-S. Kang, A. Kitoh, A. Moise, A. Turner, B. Wang, and T. Zhou, 2013: The Asian summer monsoon: An intercomparison of CMIP5 vs. CMIP3 simulations of the late 20th century. *Climate Dyn.*, **41**, 2711–2744.

Stark, J. D., C. J. Donlon, M. J. Martin, and M. E. McCulloch, 2007: OSTIA: An operational, high resolution, real time, global sea surface temperature analysis system. *Oceans 2007 - Europe*, Aberdeen, Scotland, IEEE, Vols. 1–3, 331–334, doi:10.1109/OCEANSE.2007.4302251.

Stocker, T. F., and Coauthors, Eds., 2014: *Climate Change 2013: The Physical Science Basis*. Cambridge University Press, 1535 pp.

Stone, D. A., and M. R. Allen, 2005: Attribution of global surface warming without dynamical models. *Geophys. Res. Lett.*, **32**, L18711, doi:10.1029/2005GL023682.

——, ——, P. A. Stott, P. Pall, S.-K. Min, T. Nozawa, and S. Yukimoto, 2009: The detection and attribution of human influence on climate. *Ann. Rev. Environ. Res.*, **34**, 1–16.

Stott, P. A., D. A. Stone, and M. R. Allen, 2004: Human contribution to the European heatwave of 2003. *Nature*, **432**, 610–614, doi:10.1038/nature03089.

Sutton, R. T., and B.-W. Dong, 2012: Atlantic Ocean influence on a shift in European climate in the 1990s. *Nature Geosci.*, **5**, 788–792, doi:10.1038/ngeo1595.

——, and P. P. Mathieu, 2002: Response of the atmosphere–ocean mixed-layer system to anomalous ocean heat-flux convergence. *Quart. J. Roy. Meteor. Soc.*, **128**, 1259–1275.

Swart, N. C., and J. C. Fyfe, 2012: Observed and simulated changes in the Southern Hemisphere surface westerly wind-stress. *Geophys. Res. Lett.*, **39**, L16711, doi:10/1029/2012GL052810.

Tait, A., R. Henderson, R. Turner, and X. Zheng, 2006: Thin plate smoothing spline interpolation of daily rainfall for New Zealand using a climatological rainfall surface. *Int. J. Climatol.*, **26**, 2097–2115.

Taylor, K. E., R. J. Stouffer, and G. A. Meehl, 2012: An overview of CMIP5 and the experiment design. *Bull. Amer. Meteor. Soc.,* **93**, 485–498.

Thompson, D. W. J., S. Solomon, P. J. Kushner, M. H. England, K. M. Grise, and D. J. Karoly, 2011: Signatures of the Antarctic ozone hole in Southern Hemisphere surface climate change. *Nature Geosci.*, **4**, 741–749, doi:10.1038/ngeo1296.

Trenberth, K. E., 2011: Changes in precipitation with climate change. *Climate Res.*, **47**, 123–138.

——, G. Branstator, and P. Arkin, 1988: Origins of the 1988 American drought. *Science*, **242**, 1640–1645.

——, A. Dai, G. van der Schrier, P. D. Jones, J. Barichivich, K. R. Briffa, and J. Sheffield, 2014: Global warming and changes in drought. *Nature Climate Change*, **4**, 17–22.

Trewin, B., 2012: A daily homogenized temperature data set for Australia. *Int. J. Climatol.*, **33**, 1510–1529, doi:10.1002/joc.3530.

Trigo, R. M., and Coauthors, 2013: The record winter drought of 2011-12 in the Iberian Peninsula [in "Explaining Extreme Events of 2012 from a Climate Perspective"]. *Bull. Amer. Meteor. Soc.*, **94** (9), S41–S45.

Uccellini, L. W., and P. J. Kocin, 1987: The interaction of jet streak circulations during heavy snow events along the East Coast of the United States. *Wea. Forecasting*, **2**, 289–308.

Ullah, K., and G. Shouting, 2013: A diagnostic study of convective environment leading to heavy rainfall during the summer monsoon 2010 over Pakistan. *Atmos. Res.*, **120–121**, 226–239.

USBR, 2014: Reclamation announces initial 2014 Central Valley Project water supply allocation. United States Bureau of Reclamation, news release, 21 February 2014. [Available online at http://www.usbr.gov/newsroom/newsrelease/detail.cfm?RecordID=46045.]

USDA, 2014a: Obama Administration announces additional assistance to Californians impacted by drought. United States Department of Agriculture, news release, 0022.14. [Available online at http://www.usda.gov/wps/portal/usda/usdamediafb?contentid=2014/02/0022.xml&printable=true&contentidonly=true.]

——, 2014b: Secretarial Disaster Designations - 2014 Crop Year. All Crop - Total Counties by State (updated 9/3/2014). United States Department of Agriculture. [Available online at http://www.usda.gov/documents/2014-all-crop-list-counties.pdf.]

USGS, cited 2014: California Water Science Center. [Available online at http://ca.water.usgs.gov/data/drought/drought-impact.html.]

van Haren, R., G. J. van Oldenborgh, G. Lenderink, and W. Hazeleger, 2013a: Evaluation of modeled changes in extreme precipitation in Europe and the Rhine basin. *Environ. Res. Lett.*, **8**, 014053, doi:10.1088/1748-9326/8/1/014053.

——, ——, ——, M. Collins, and W. Hazeleger, 2013b: SST and circulation trend biases cause an underestimation of European precipitation trends. *Climate Dyn.*, **40**, 1–20.

van Oldenborgh, G. J., A. van Urk, and M. Allen, 2012: The absence of a role of climate change in the 2011 Thailand floods. *Bull. Amer. Meteor. Soc.*, **93**, 1047–1049.

——, F. J. Doublas Reyes, S. S. Dirjfhout, and E. Hawkins, 2013: Reliability of regional climate model trends. *Environ. Res. Lett.*, **8**, 014055, doi:10.1088/1748-9326/8/1/014055.

Vautard, R., and P. Yiou, 2009: Control of recent European surface climate change by atmospheric flow. *Geophys. Res. Lett.*, **36**, L22702, doi:10.1029/2009GL040480.

——, and Coauthors, 2007: Summertime European heat and drought waves induced by wintertime Mediterranean rainfall deficit. *Geophys. Res. Lett.*, **34**, L07711, doi:10.1029/2006GL028001.

VegDRI, cited 2014: Vegetation drought response index. [Available online at http://vegdri.unl.edu/.]

Vicente-Serrano, S. M., R. M. Trigo, J. I. López-Moreno, M. L. R. Liberato, J. Lorenzo-LaCruz, S. Beguería, E. Morán-Tejada, and A. El Kenawy, 2011: Extreme winter precipitation in the Iberian Peninsula in 2010: Anomalies, driving mechanisms and future projections. *Climate Res.*, **46**, 51–65.

Visbeck, M. H., J. W. Hurrell, L. Polvani, and H. M. Cullen, 2001: The North Atlantic Oscillation: Past, present, and future. *Proc. Natl. Acad. Sci. USA*, **98**, 12876–12877.

Vose, R. S., R. L. Schmoyer, P. M. Steurer, T. C. Peterson, R. Heim, T. R. Karl, and J. K. Eischeid, 1992: The Global Historical Climatology Network: Long-term monthly temperature, precipitation, sea level pressure, and station pressure data. ORNL/CDIAC-53, NCDP-041, 325 pp.

——, and Coauthors, 2014: Improved historical temperature and precipitation time series for U.S. climate divisions. *J. App. Meteor. Climatol.*, **53**, 1232–1251.

Wakabayashi, S., and R. Kawamura, 2004: Extraction of major teleconnection patterns possibly associated with the anomalous summer climate in Japan. *J. Meteor. Soc. Japan*, **82**, 1577–1588.

Wallace, J. M., I. M. Held, D. W. J. Thompson, K. E. Trenberth, and J. E. Walsh, 2014: Global warming and winter weather. *Science*, **343**, 729–730, doi:10.1126/science.343.6172.729.

Wang, B., B. Xiang, and J.-Y. Lee, 2013: Subtropical high predictability establishes a promising way for monsoon and tropical storm predictions. *Proc. Natl. Acad. Sci. USA*, **110**, 2718–2722.

Wang, S.-Y., R. E. Davies, W.-R. Huang, and R. R. Gillies, 2011: Pakistan's two-stage monsoon and links with the recent climate change. *J. Geophys. Res.*, **116**, D16114, doi:10.1029/2011JD015760.

——, L. Hipps, R. R. Gillies, and J.-H. Yoon, 2014: Probable causes of the abnormal ridge accompanying the 2013–2014 California drought: ENSO precursor and anthropogenic warming footprint. *Geophys. Res. Lett.*, **41**, 3220–3226, doi:10.1002/2014GL059748.

Watanabe, M., and Coauthors, 2010: Improved climate simulation by MIROC5: Mean states, variability, and climate sensitivity. *J. Climate*, **23**, 6312–6335.

Water CA, cited 2014: California Department of Water Resources. [Available online at http://www.water.ca.gov/waterconditions/.]

Webster, P. J., V. O. Magaña, T. N. Palmer, J. Shukla, R. A. Tomas, M. Yanai, and T. Yasunari, 1998: Monsoons: Processes, predictability, and the prospects for prediction. *J. Geophys. Res.*, **103** (C7), 14451–14510, doi:10.1029/97JC02719.

——, V. E. Toma, and H.-M. Kim, 2011: Were the 2010 Pakistan floods predictable? *Geophys. Res. Lett.*, **38**, L04806, doi:10.1029/2010GL046346.

Weisse, R., H. von Storch, and F. Feser, 2005: Northeast Atlantic and North Sea storminess as simulated by a regional climate model during 1958-2001 and comparison with observations. *J. Climate*, **18**, 465–479.

Wen, Q. H., X. Zhang, Y. Xu, and B. Wang, 2013: Detecting human influence on extreme temperatures in China. *Geophys. Res. Lett.*, **40**, 1171–1176, doi:10.1002/grl.50285.

Westra, S., L. V. Alexander, and F. W. Zwiers, 2013: Global increasing trends in annual maximum daily precipitation. *J. Climate*, **26**, 3904–3918.

Wheeler, M. C., and H. H. Hendon, 2004: An all season real-time multivariate MJO index: Development of an index for monitoring and prediction. *Mon. Wea. Rev.*, **132**, 1917–1932.

Wilks, D. S. 2006: *Statistical Methods in the Atmospheric Sciences.* International Geophysics Series, Vol. 91, Elsevier Academic Press, 627 pp.

WMO, 2010: Guide to meteorological instruments and methods of observation. WMO No. 8. World Meteorological Society, 437 pp. [Available online at http://www.wmo.int/pages/prog/www/IMOP/CIMO-Guide.html.]

——, 2013: The state of greenhouse gases in the atmosphere based on global observations through 2012. *WMO Greenhouse Gas Bulletin*, No. 9, 4 pp.

Wu, G., Y. Liu, B. He, Q. Bao, A. Duan, and F.-F. Jin, 2012: Thermal controls on the Asian summer monsoon. *Sci. Rep.*, **2**, Article 404, doi:10.1038/srep00404.

Wu, L., and Coauthors, 2012: Enhanced warming over the global subtropical western boundary currents. *Nature Climate Change*, **29**, 161–166.

Xavier, P. K., C. Marzin, and B. N. Goswami, 2007: An objective definition of the Indian summer monsoon season and a new perspective on the ENSO–monsoon relationship. *Quart. J. Roy. Meteor. Soc.,* **133**, 749–764.

Yiou, P., and J. Cattiaux, 2013: Contribution of atmospheric circulation to wet north European summer precipitation of 2012[in "Explaining Extreme Events of 2012 from a Climate Perspective"]. *Bull. Amer. Meteor. Soc.*, **94** (9), S39–S41.

——, R. Vautard, P. Naveau, and C. Cassou, 2007: Inconsistency between atmospheric dynamics and temperatures during the exceptional 2006/2007 fall/winter and recent warming in Europe. *Geophys. Res. Lett.*, **34**, L21808, doi:10.1029/2007GL031981.

——, K. Goubanova, Z. X. Li, and M. Nogaj, 2008: Weather regime dependence of extreme value statistics for summer temperature and precipitation. *Nonlin. Processes Geophys.*, **15**, 365–378, doi:10.5194/npg-15-365-2008.

Yu, R., and T. Zhou, 2007: Seasonality and three-dimensional structure of the interdecadal change in East Asian monsoon. *J. Climate*, **20**, 5344–5355.

——, B. Wang, and T. Zhou, 2004: Tropospheric cooling and summer monsoon weakening trend over East Asia. *Geophys. Res. Lett.*, **31**, L22212, doi:10.1029/2004GL021270.

Zhang, X., F. W. Zwiers, G. C. Hegerl, F. H. Lambert, N. P. Gillett, S. Solomon, P. A. Stott, and T. Nozawa, 2007: Detection of human influence on twentieth-century precipitation trends. *Nature*, **448**, 461–465.

——, H. Wan, F. W. Zwiers, G. C. Hegerl, and S.-K. Min, 2013: Attributing intensification of precipitation extremes to human influence. *Geophys. Res. Lett.*, **40**, 5252–5257, doi:10.1002/grl.51010.

Zhou, T., D. Gong, J. Li, and B. Li, 2009: Detecting and understanding the multi-decadal variability of the East Asian Summer Monsoon - Recent progress and state of affairs. *Meteor. Z.*, **18**, 455–467.

——, F. Song, R. Lin, X. Chen, and X. Chen, 2013: The 2012 North China floods: Explaining an extreme rainfall event in the context of a long-term drying tendency [in "Explaining Extreme Events of 2012 from a Climate Perspective"]. *Bull. Amer. Meteor. Soc.*, **94** (9), S49–S51.

Zolina, O., C. Simmer, A. Kapala, P. Shabanov, P. Becker, H. Mächel, S. Gulev, and P. Groisman, 2013: New view on precipitation variability and extremes in Central Europe from a German high resolution daily precipitation dataset: Results from STAMMEX project *Bull. Amer. Meteor. Soc.*, **95**, 995–1002.

Zwiers, F. W., X. Zhang, and Y. Feng, 2011: Anthropogenic influence on long return period daily temperature extremes at regional scales. *J. Climate*, **24**, 881–892.

REFERENCES FOR SUPPLEMENTAL MATERIAL

Adler, R. F., and Coauthors, 2003: The Version 2 Global Precipitation Climatology Project (GPCP) monthly precipitation analysis (1979-Present). *J. Hydrometeor.*, **4**, 1147–1167.

Becker, A., P. Finger, A. Meyer-Christoffer, B. Rudolf, K. Schamm, U. Schneider, and M. Ziese, 2013: A description of the global land-surface precipitation data products of the Global Precipitation Climatology Centre with sample applications including centennial (trend) analysis from 1901 to present. *Earth Syst. Sci. Data,* **5**, 71–99.

Benjamini, Y., and Y. Hochberg, 1995: Controlling the false discovery rate: A practical and powerful approach to multiple testing. *J. Roy. Stat. Soc.*, **B57**, 289–300.

Bindoff, N. L., and Coauthors, 2013: Detection and attribution of climate change: From global to regional. *Climate Change 2013: The Physical Science Basis*, T. F. Stocker et al., Eds., Cambridge University Press, 867–952.

Borah, N., A. K. Sahai, R. Chattopadhyay, S. Joseph, S. Abhilash, and B. N. Goswami, 2013: A self-organizing map–based ensemble forecast system for extended range prediction of active/break cycles of Indian summer monsoon. *J. Geophys. Res. Atmos.*, **118**, 9022–9034, doi:10.1002/jgrd.50688.

Bureau of Meteorology, 2013: Australia's warmest September on record. Bureau of Meteorology Special Climate Statement 46, 26 pp. [Available online at http://www.bom.gov.au/climate/current/statements/scs46.pdf.]

Cassou, C., 2008: Intraseasonal interaction between the Madden–Julian Oscillation and the North Atlantic Oscillation. *Nature*, **455**, 523–527.

Chattopadhyay, R., A. K. Sahai, and B. N. Goswami, 2008: Objective identification of nonlinear convectively coupled phases of monsoon intraseasonal oscillation: Implications for prediction. *J. Atmos. Sci.*, **65**, 1549–1569.

Chen, S., and D. Cayan, 1994: Low-frequency aspects of the large-scale circulation and West Coast United States temperature/precipitation fluctuations in a simplified general circulation model. *J. Climate*, **7**, 1668–1683.

Christiansen, B., 2013: Changes in temperature records and extremes: are they statistically significant? *J. Climate,* **26**, 7863–7875.

Christidis, N., and P. A. Stott, 2014: Change in the odds of warm years and seasons due to anthropogenic influence on the climate. *J. Climate*, **27**, 2607–2621.

—, —, A. Scaife, A. Arribas, G. S. Jones, D. Copsey, J. R. Knight, and W. J. Tennant, 2013: A new HadGEM3-A based system for attribution of weather and climate-related extreme events. *J. Climate*, **26**, 2756–2783.

Compo, G. P., and P. D. Sardeshmukh, 2010: Removing ENSO-related variations from the climate record. *J. Climate*, **23**, 1597–1978.

Dash, S. K., M. A. Kulkarni, U. C. Mohanty, and K. Prasad, 2009: Changes in the characteristics of rain events in India. *J. Geophys. Res.*, **114**, D10109, doi:10.1029/2008jd010572.

Dee, D. P., and Coauthors, 2011: The ERA-Interim reanalysis: configuration and performance of the data assimilation system. *Quart. J. Roy. Meteor. Soc.*, **137**, 553–597, doi:10.1002/qj.828.

Dong, B.-W., R. T. Sutton, and T. Woollings, 2013: The extreme European summer 2012 [in "Explaining Extreme Events of 2012 from a Climate Perspective"]. *Bull. Amer. Meteor. Soc.,* **94** (9), S28–S32.

Feldstein, S. B., 2000: The timescale, power spectra, and climate noise properties of teleconnection patterns. *J. Climate*, **13**, 4430–4440.

Flato, G., and Coauthors, 2013: Evaluation of climate models. *Climate Change 2013: The Physical Science Basis,* T. F. Stocker et al., Eds., Cambridge University Press, 741–866.

Galloway, J. M., A. Wigston, R.T. Patterson, G.T. Swindles, E. Reinhardt, H.M. Roe, 2013: Climate change and decadal to centennial-scale periodicities recorded in a late Holocene NE Pacific marine record: Examining the role of solar forcing. *Palaeogeogr., Palaeoclimatol., Palaeoecol.*, **386**, 669–689.

Ghosh, S., D. Das, S.-C. Kao, and A. R. Ganguly, 2012: Lack of uniform trends but increasing spatial variability in observed Indian rainfall extremes. *Nature Climate Change*, **2**, 86–91, doi:10.1038/nclimate1327.

Hewitson, B. C., and R. G. Crane, 2002: Self-organizing maps: Applications to synoptic climatology. *Climate Res.*, **22**, 13–26.

Hewitt, H. T., D. Copsey, I. D. Culverwell, C. M. Harris, R. S. R. Hill, A. B. Keen, A. J. McLaren, and E. C. Hunke, 2011: Design and implementation of the infrastructure of HadGEM3: the next-generation Met Office climate modelling system. *Geosci. Model Dev.*, **4**, 223–253.

Hudson, D., A. G. Marshall, Y. Yin, O. Alves and H. H. Hendon, 2013: Improving intraseasonal prediction with a new ensemble generation strategy. *Mon. Wea. Rev.*, **141**, 4429–4449.

Hurrell, J., and Coauthors, 2013: The Community Earth System Model: A framework for collaborative research. *Bull. Amer. Meteor. Soc.*, **94**, 1339–1360.

Johnson, N. C., 2013: How many ENSO flavors can we distinguish? *J. Climate*, **26**, 4816–4827.

—, S. B. Feldstein, and B. Tremblay, 2008: The continuum of Northern Hemisphere teleconnection patterns and a description of the NAO Shift with the use of self-organizing maps. *J. Climate*, **21**, 6354–6371.

Jones, D. A., W. Wang, and R. Fawcett, 2009: High-quality spatial climate data-sets for Australia. *Aust. Meteor. Ocean. J.*, **58**, 233–248.

Kalnay, E., and Coauthors, 1996: The NCEP/NCAR 40-Year Reanalysis Project. *Bull. Amer. Meteor. Soc.*, **77**, 437–471.

Knutson, T. R., F. Zeng, and A. T. Wittenberg, 2013: Multimodel assessment of regional surface temperature trends: CMIP3 and CMIP5 Twentieth Century simulations. *J. Climate*, **26**, 8709–8743.

Kohonen, T., 2001: *Self-Organizing Maps*. 3rd ed. Springer Series in Information Sciences, Vol. 30, Springer, 501 pp.

Lewis, S. C., and D. J. Karoly, 2013: Anthropogenic contributions to Australia's record summer temperatures of 2013. *Geophys. Res. Lett.*, **40**, 3705–3709, doi:10.1002/grl.50673.

Lim, E.-P., H. H. Hendon, D. L. T. Anderson, and A. Charles, 2011: Dynamical, statistical-dynamical, and multimodel ensemble forecasts of Australian spring season rainfall. *Mon. Wea. Rev.,* **139**, 958–975.

Liu, Y., R. H. Weisberg, and C. N. K. Mooers, 2006: Performance evaluation of the self-organizing map for feature extraction. *J. Geophys. Res.*, **111**, C05018, doi:10.1029/2011GL047658.

Livezey, R. E., and W. Y. Chen, 1983: Statistical field significance and its determination with Monte Carlo techniques. *Mon. Wea. Rev.*, **111**, 46–59.

Mastrandrea, M. D., K. J. Mach, G.-K. Plattner, O. Edenhofer, T. F. Stocker, C. B. Field, K. L. Ebi, and P. R. Matschoss, 2011: The IPCC AR5 guidance note on consistent treatment of uncertainties: A common approach across the working groups. *Climatic Change*, **108**, 675–691.

Mitchell, T., and W. Blier, 1997: The variability of wintertime precipitation in the region of California. *J. Climate*, **10,** 2261–2276.

Mo, R., and D. M. Straus, 2002: Statistical–dynamical seasonal prediction based on principal component regression of GCM ensemble integrations. *Mon. Wea. Rev.*, **130**, 2167–2187.

Morice, C. P., J. J. Kennedy, N. A. Rayner, and P. D. Jones, 2012: Quantifying uncertainties in global and regional temperature change using an ensemble of observational estimates: The HadCRUT4 dataset. *J. Geophys. Res.*, **117**, D08101, doi:10.1029/2011JD017187.

Moss, R. H., and Coauthors, 2010: The next generation of scenarios for climate change research and assessment. *Nature*, **463**, 747–756.

Murphy, J. M., D. M. H. Sexton, D. N. Barnett, G. S. Jones, M. J. Webb, M. Collins, and D. A. Stainforth, 2004: Quantification of modelling uncertainties in a large ensemble of climate change simulations. *Nature*, **430**, 768–772.

Pall, P., T. Aina, D. A. Stone, P. A. Stott, T. Nozawa, A. G. J. Hilberts, D. Lohmann, and M. R. Allen, 2011: Anthropogenic greenhouse gas contribution to flood risk in England and Wales in autumn 2000. *Nature*, **470**, 382–385.

Park, S., and C. S. Bretherton, 2009: The University of Washington shallow convection and moist turbulence schemes and their impact on climate simulations with the Community Atmosphere Model. *J. Climate*, **22**, 3449–3469.

Polade, S. D., A. Gershunov, D. R. Cayan, M. D. Dettinger and D. W. Pierce, 2013: Natural climate variability and teleconnections to precipitation over the Pacific-North American region in CMIP3 and CMIP5 models. *Geophys. Res. Lett.*, **40**, 2296–2301, doi:10.1002/grl.50491.

Porteous, A., and B. Mullan, 2013: The 2012-13 drought: An assessment and historical perspective. MPI Tech. Paper No. 2012/18, Ministry for Primary Industries/ National Institute of Water & Atmospheric Research, 57 pp. [Available online at http://www.niwa.co.nz/sites/niwa.co.nz/files/2013-18-The%202012-13%20drought%20an%20assessment%20and%20historical%20perspective.pdf.]

Rajeevan, M., J. Bhate, J. Kale, and B. Lal, 2006: A high resolution daily gridded rainfall for the Indian region: Analysis of break and active monsoon spells. *Current Sci.*, **91**, 296–306.

—, S. Gadgil, and J. Bhate, 2010: Active and break spells of the Indian summer monsoon. *J. Earth Sys. Sci.*, **119**, 229–247, doi:10.1007/s12040-010-0019-4.

Raupach, M. R., P. R. Briggs, V. Haverd, E. A. King, M. Paget, and C. M. Trudinger, 2009: Australian Water Availability Project (AWAP): CSIRO Marine and Atmospheric Research Component: Final Report for Phase 3. CAWCR Technical Report No.013, 67 pp.

Reusch, D. B., R. B. Alley, and B. C. Hewitson, 2005: Relative performance of self-organizing maps and principal component analysis in pattern extraction from synthetic climatological data. *Polar Geogr.*, **29**, 188–212.

Reynolds, R. W., N. A. Rayner, T. M. Smith, D. C. Stokes, and W. Wang, 2002: An improved in situ and satellite SST analysis for climate. *J. Climate*, **15**, 1609–1625.

Saji, N. H., B. N. Goswami, P. N. Vinayachandran, and T. Yamagata, 1999: A dipole mode in the tropical Indian Ocean. *Nature*, **401**, 360–363.

Shin, S., and P. D. Sardeshmukh, 2011: Critical influence of the pattern of tropical ocean warming on remote climate trends. *Climate Dyn.*, **36**, 1577–1591.

Singh, C., 2013: Characteristics of monsoon breaks and intraseasonal oscillations over central India during the last half century. *Atmos. Res.*, **128**,120–128, doi:10.1016/j.atmosres.2013.03.003.

Slingo, J., 2013: Why was the start to spring 2013 so cold? Met Office briefing note, April 2013. [Available online at http://www.metoffice.gov.uk/research/news/cold-spring-2013.]

Smith, T. M., R. W. Reynolds, T. C. Peterson, and J. Lawrimore, 2008: Improvements to NOAA's Historical Merged Land-Ocean Surface Temperature analysis (1880-2006). *J. Climate*, **21**, 2283–2296.

Solomon, A., and M. Newman, 2012: Reconciling disparate twentieth-century Indo-Pacific ocean temperature trends in the instrumental record. *Nature Climate Change*, **2**, 691–699.

Sperber, K. R., H. Annamalai, I.-S. Kang, A. Kitoh, A. Moise, A. Turner, B. Wang, and T. Zhou, 2013: The Asian summer monsoon: An intercomparison of CMIP5 vs. CMIP3 simulations of the late 20th century. *Climate Dyn.*, **41**, 2711–2744.

Stark, J. D., C. J. Donlon, M. J. Martin, and M. E. McCulloch, 2007: OSTIA: An operational, high resolution, real time, global sea surface temperature analysis system. *Oceans 2007 - Europe*, Aberdeen, Scotland, IEEE, Vols. 1–3, 331–334, doi:10.1109/OCEANSE.2007.4302251.

Stott, P. A., G. S. Jones, J. A. Lowe, P. Thorne, C. F. Durman, T. C. Johns, and J.-C. Thelen, 2006: Transient climate simulations with the HadGEM1 climate model: Cases of past warming and future climate change. *J. Climate*, **19**, 2763–2782.

Taylor, K. E., R. J. Stouffer, and G. A. Meehl, 2012: An overview of CMIP5 and the experiment design. *Bull. Amer. Meteor. Soc.*, **93**, 485–498.

Tennant, W. J., G. J. Shutts, A. Arribas, and S. A. Thompson, 2011: Using a stochastic kinetic energy backscatter scheme to improve MOGREPS probabilistic forecast skill. *Mon. Wea. Rev.*, **139**, 1190–1206.

White, C. J., D. Hudson, and O. Alves, 2014: ENSO, the IOD and the intraseasonal prediction of heat extremes across Australia using POAMA-2. *Climate Dyn.*, doi:10.1007/s00382-013-2007-2.

Wilks, D. S., 2006: On "field significance" and the false discovery rate. *J. Appl. Meteor. Climatol.*, **45**, 1181–1189.

Zanchettin, D., A. Rubino, and J. H. Jungclaus, 2010: Intermittent multidecadal-to-centennial fluctuations dominate global temperature evolution over the last millennium. *Geophys. Res. Lett.*, **37**, L14702, doi:10.1029/2010GL043717.

Zhang, G. J., and N. A. McFarlane, 1995: Sensitivity of climate simulations to the parameterization of cumulus convection in the Canadian Climate Centre general circulation model. *Atmos.—Ocean*, **33**, 407–446.